

Store-Operated Calcium Entry as a Therapeutic Target in Acute Pancreatitis: Discovery and Development of Drug-Like SOCE Inhibitors

Marta Serafini, Celia Cordero-Sanchez, Rosanna Di Paola, Irene P. Bhela, Silvio Aprile, Beatrice Purghe, Roberta Fusco, Salvatore Cuzzocrea, Armando A. Genazzani, Beatrice Riva, and Tracey Pirali*

Cite This: *J. Med. Chem.* 2020, 63, 14761–14779

Read Online

ACCESS |



Metrics & More

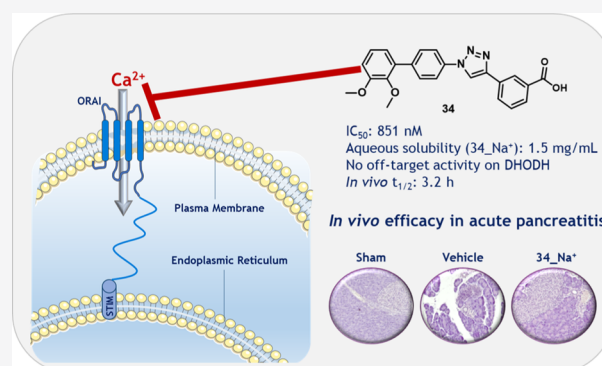


Article Recommendations



Supporting Information

ABSTRACT: Store-operated calcium entry (SOCE) is important in the maintenance of calcium homeostasis and alterations in this mechanism are responsible for several pathological conditions, including acute pancreatitis. Since the discovery of SOCE, many inhibitors have been identified and extensively used as chemical probes to better elucidate the role played by this cellular mechanism. Nevertheless, only a few have demonstrated drug-like properties so far. Here, we report a class of biphenyl triazoles among which stands out a lead compound, **34**, that is endowed with an inhibitory activity at nanomolar concentrations, suitable pharmacokinetic properties, and *in vivo* efficacy in a mouse model of acute pancreatitis.



INTRODUCTION

Acute pancreatitis (AP) is an inflammatory life-threatening disorder. It is characterized by autodigestion of the pancreas, which causes inflammation, edema, vacuolization, necrosis, and, in the worst scenario, induces injury of remote extrapancreatic organs. AP represents an urgent and unmet need as it affects about 35 individuals per 100,000 person-years worldwide,¹ with a mortality rate between 1.5 and 4.2%, and no effective pharmacological treatment is available.^{1,2}

Among the triggers of AP is an intracellular Ca²⁺ overload in pancreatic acinar cells (PACs) that induces the uncontrolled release of intracellular digestive proenzymes. While there are numerous mechanisms that control intracellular Ca²⁺ concentrations, store-operated Ca²⁺ entry (SOCE) appears to have a pivotal role in the induction of Ca²⁺ overload in PACs.³

SOCE⁴ is represented by the influx of Ca²⁺ activated in response to the depletion of the stores from the endoplasmic reticulum (ER)⁵ and is associated with the electrophysiological current named I_{CRAC} (CRAC, calcium release-activated channel).⁶ The exact molecular mechanism behind this cellular event was elucidated between 2005 and 2006, when the principal components of SOCE machinery, STIM and Orai, were discovered.⁷ At present, three Orai isoforms (Orai1–3) and two STIM isoforms (STIM1–2) are known. STIM is a single-span protein located on the ER membrane and behaves as a sensor: the depletion of ER Ca²⁺ stores induces a conformational change of STIM that, after oligomerization, interacts with Orai. The latter is a plasma membrane Ca²⁺

channel that allows for Ca²⁺ influx from the extracellular environment, eventually refilling the intracellular Ca²⁺ stores.

Other crucial proteins known to participate in SOCE are transient receptor potential canonical (TRPC) channels,⁸ which were previously believed to be the primary contributors of Ca²⁺ rise in PACs and therefore mainly responsible for AP.^{5b,9} Yet, more recent studies have demonstrated that the metabolic alcohol products that are among the mediators of acinar cell damage induce the opening of IP₃Rs, Ca²⁺ channels located in the ER, resulting in the depletion of the ER stores and in the activation of STIM.¹⁰ This event leads to Ca²⁺ entry through the Orai1 opening, sustaining toxic intracellular Ca²⁺ elevation and pointing to Orai1 as a key culpable for AP damage.¹⁰

Gerasimenko *et al.* demonstrated that a selective CRAC channel blocker, GSK-7975A (**1**, Figure 1), with no inhibitory activity on TRP-channel currents, is able to decrease the overload of cytosolic Ca²⁺ in a concentration-dependent manner and to prevent the activation of the necrotic cell death pathway in both mouse and human PACs,¹¹ confirming the involvement of Orai in AP and its druggability.

Received: July 27, 2020

Published: November 30, 2020



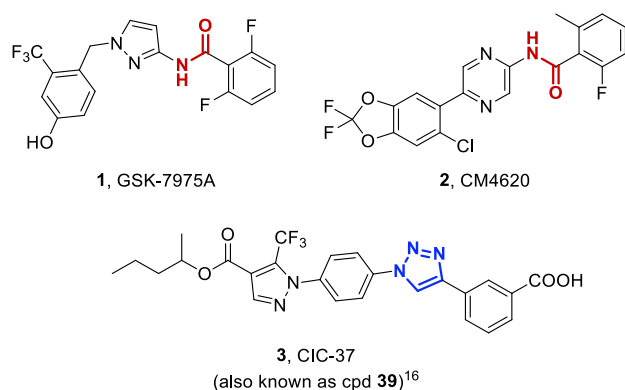


Figure 1. Negative modulators of SOCE reported in the literature.

Furthermore, GSK-7975A, together with another SOCE inhibitor, CM4620 (**2**, Figure 1), were demonstrated to be protective in three different murine models of chemically induced AP.¹² Based on these preclinical evidences, CM4620 has entered clinical trials,¹³ with a Phase II trial for AP already completed and an ongoing Phase I/II trial for a rare condition in which AP is triggered by asparaginase treatment (asparaginase-associated AP). This rare condition (incidence between 7 and 18%) is a well-known complication of childhood acute lymphoblastic leukemia (ALL) treatment that is often responsible for the early discontinuation of drug treatments.^{3b} As the increase in Ca^{2+} induced by asparaginase and the related necrosis of PACs depend on CRAC channels, recent findings have described the inhibition of CRAC channels as the most promising therapeutic approach in this pathology.^{3a,14}

Among the several medicinal chemistry campaigns aimed at developing SOCE inhibitors,¹⁵ in 2018 our research group described a class of SOCE modulators, named pytriazoles,¹⁶ that were designed based on a known chemical probe for SOCE, Pyr6.¹⁷ Among the reported compounds, a promising candidate (**3**, Figure 1) able to significantly ameliorate cerulein-induced AP in rodents without signs of toxicity was identified. Nevertheless, the pharmacokinetic (PK) profile of **3**, with its relatively short half-life (mouse, i.p., 1.3 h) and high volume of distribution (32 L/kg), prompted us to undertake a medicinal chemistry campaign aimed at developing more drug-like SOCE modulators.

Among the previously reported SOCE modulators, **Synta66** (**4**, Figure 2) is a CRAC channel blocker able to inhibit I_{CRAC} with an IC_{50} of 1.4–3.0 μM .¹⁸ Although its precise mechanism on SOCE remains unknown, assays performed in siRNA knock-down of Orai1 mast cells have suggested that **Synta66** might be selective for the channel.^{18a} Furthermore, experiments in vascular smooth muscle cells have demonstrated that it does not interfere with STIM1 clustering.¹⁹ Thanks to its inhibitory activity toward Orai1, an increasing number of *in vitro* and *in vivo* studies have used **Synta66** as a chemical probe to gain better insight into I_{CRAC} biology. Moreover, the compound is selective over a panel of other ion channels or receptors, including Ca^{2+} ATPase pump, voltage-gated Ca^{2+} and Na^{+} channels, and TRPC1/5 channels,^{18a,b,19} indicating this molecule as a reliable starting point to develop new SOCE modulators.

In the present contribution, we describe a family of biphenyl triazoles that inhibit SOCE and are endowed with potency in the nanomolar range, good PK profile, and efficacy in

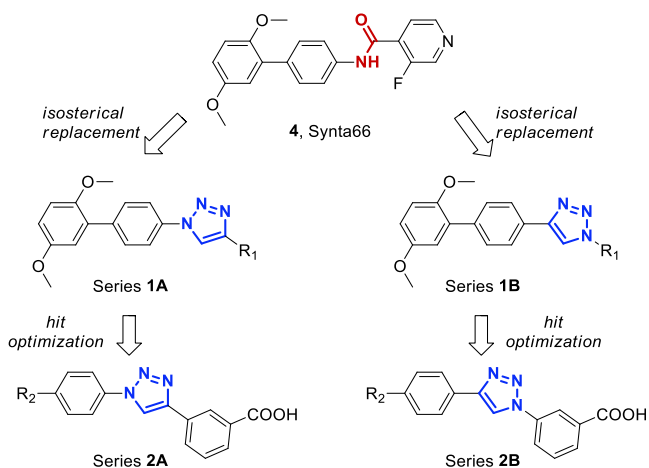


Figure 2. Modifications of **Synta66** moieties to synthesize biphenyl triazoles.

counteracting cerulein-induced AP. While the compounds had been initially designed as mere isosteres of **Synta66**,²⁰ replacement of the arylamide moiety with the triazole ring (Figure 2) gave unpredictable results in terms of structure–activity relationships (SARs) and unmasked the fact that this represents a completely new class of modulators.

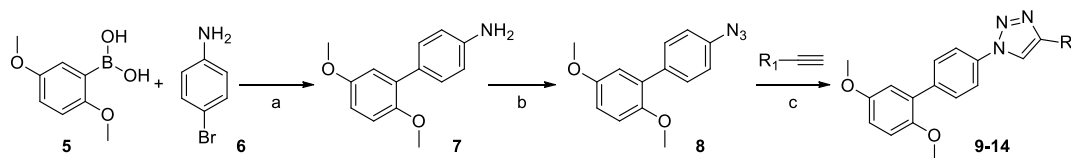
RESULTS AND DISCUSSION

SAR Study around 2-Fluoro-4-pyridine Gives Less-Active Compounds Compared to **Synta66** on SOCE.

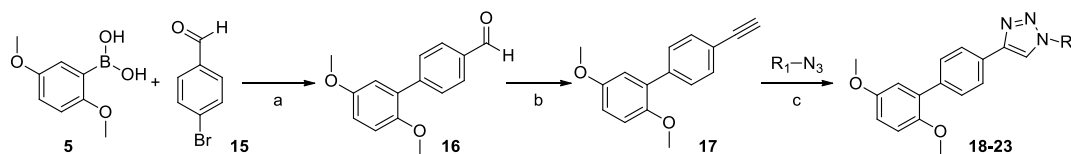
Starting from the structure of **Synta66**, the amide moiety was replaced with a 1,4-disubstituted 1,2,3-triazole ring by a click chemistry approach.²¹ To this aim, azide **8** and alkyne **17** were prepared according to Schemes 1 and 2. **8** was synthesized starting from (2,5-dimethoxyphenyl)boronic acid and 4-bromoaniline, which reacted in a Suzuki cross-coupling reaction to give intermediate **7**. Compound **7** underwent a diazotization-azidation reaction to afford the desired azide **8** with a yield of 60%. Alkyne **17** was prepared from (2,5-dimethoxyphenyl)boronic acid and 4-bromobenzaldehyde, which, after a Suzuki cross-coupling reaction, gave intermediate **16** that reacted in the presence of Bestmann–Ohira reagent to give **17**.

With these two compounds in hand, two click reactions were performed and compounds **9** and **18** (Table 1), displaying the same substructures as the reference compound **Synta66**, were obtained with a yield of 31 and 60%, respectively. **9** and **18** were tested for activity on SOCE in HEK cells, a human embryonic kidney (HEK) cell line, by fluorescence microscopy, as described elsewhere.¹⁶ After 600 s, Ca^{2+} was added and intracellular levels were measured. Compared to **Synta66**, which exhibits an inhibition of $90.8 \pm 1.7\%$, compound **18** inhibited SOCE to a smaller extent ($26.2 \pm 6.5\%$), whereas **9** showed a percentage of -4.9 ± 21.3 , indicating that the molecule slightly increased Ca^{2+} entry compared to control (Table 1). Therefore, the isosteric replacement of the aryl amide moiety with a triazole ring led to active molecules, although the activity was significantly reduced compared to the parent compound **Synta66**.

Prompted by this observation, we decided to investigate the SAR around the 2-fluoro-4-pyridine ring. To this aim, 10 additional molecules were designed and synthesized starting from azide **8** and alkyne **17** that were clicked with five different

Scheme 1. Synthesis of Compounds 9–14 (Series 1A)^a

^aReagents and conditions: (a) K_2CO_3 , $Pd(OAc)_2$, EtOH, DMF, 80 °C, 3 h, 98%. (b) $NaNO_2$, NaN_3 , HCl, H_2O , rt, 5 h, 60%. (c) Sodium ascorbate, $CuSO_4 \cdot 5H_2O$, *t*-BuOH, H_2O , 50 °C, 16 h, 31–65%.

Scheme 2. Synthesis of Compounds 18–23 (Series 1B)^a

^aReagents and conditions: (a) K_2CO_3 , $Pd(OAc)_2$, EtOH, DMF, 50 °C, 3 h, 99%. (b) Bestmann–Ohira reagent, K_2CO_3 , MeOH, rt, 18 h, 82%. (c) Sodium ascorbate, $CuSO_4 \cdot 5H_2O$, *t*-BuOH, H_2O , 50 °C, 16 h, 60–99%.

Table 1. First Series of Compounds and Their Biological Activity in HEK Cells

series 1A					series 1B				
Cpd, Yield (%)	R ₁	% SOCE inhibition (10 μM)	% Viability (10 μM)	IC ₅₀ (nM)	Cpd, Yield (%)	R ₁	% SOCE inhibition (10 μM)	% Viability (10 μM)	IC ₅₀ (nM)
4, Synta66	-	90.8 ± 1.7	75.8 ± 8.0	228 ± 33					
9, 31%		-4.9 ± 21.3	-	-	18, 60%		26.2 ± 6.5	-	-
10, 37%		-12.8 ± 14.4	-	-	19, 79%		-1.7 ± 12.6	-	-
11, 65%		-14.0 ± 31.9	-	-	20, 78%		1.2 ± 33.4	-	-
12, 50%		0.0 ± 1.5	-	-			73.5 ± 1.4	-	-
13, 58%		79.9 ± 4.1	-	-	22, 75%		57.2 ± 8.3	-	-
14, 42%		76.2 ± 5.2	-	-	23, 99%		87.8 ± 2.9	71.8 ± 0.5	1790 ± 143

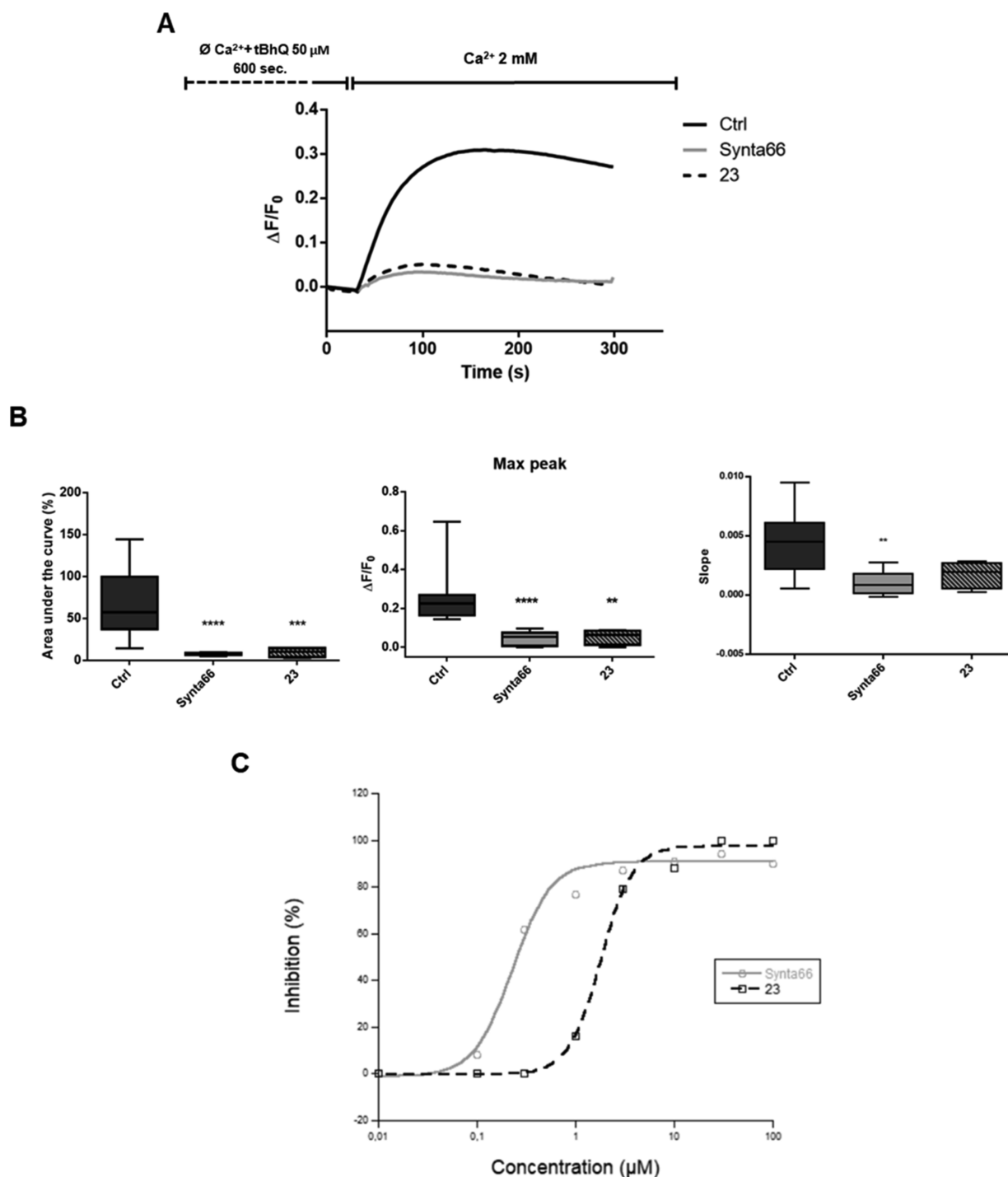
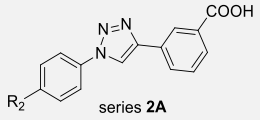
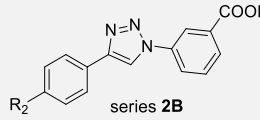
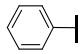
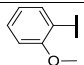
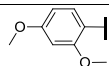
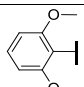
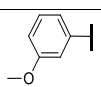
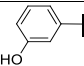
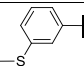
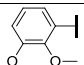
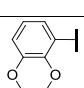
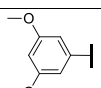
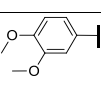
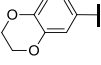
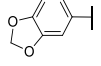
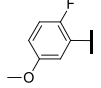


Figure 3. Effect of **Synta66** (**4**) and **23** on SOCE in HEK cells. (A) Average Ca²⁺-traces of SOCE in the absence or presence of **Synta66** or **23** (10 μM). Traces are the average of 200 cells. (B) Evaluation of the AUC, peak amplitude, and slope of the Ca²⁺-rise of the Ca²⁺-traces in the absence or presence of **Synta66** or **23**. The graph shows the median and IQR of the AUC, peak amplitude, and slope of the Ca²⁺-rise. Mann–Whitney *U* test of compounds vs control (***p* < 0.0075 ****p* = 0.0002 *****p* < 0.0001). (C) Concentration–response curves of **Synta66** and **23**.

alkynes and azides, respectively, affording compounds **10–14** (series 1A, Figure 2) and **19–23** (series 1B, Figure 2). All the synthesized triazoles were tested as described above. Five compounds (**9**, **10**, **11**, **19**, **20**) evoked a variable Ca²⁺ entry, leading to a remarkable standard error and suggesting that they were not able to reliably inhibit SOCE (Table 1). Moreover, only four molecules (**13**, **14**, **21**, **23**) out of 12 inhibited SOCE by a considerable level (arbitrarily chosen to be >70%).

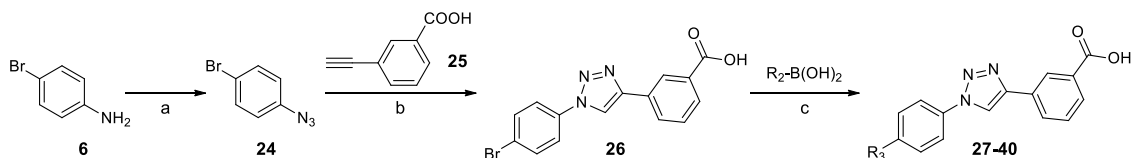
The most active compound, **23** (87.8 ± 2.9% of inhibition) showed an inhibitory activity comparable to **Synta66** (90.8 ± 1.7%; Figure 3A). The effects of both compounds on SOCE were characterized analyzing the area under the curve (AUC), peak amplitude, and slope. As shown in Figure 3B, both **Synta66** and **23** significantly reduced AUC and peak amplitude compared to control. Whereas only **Synta66** showed a significant effect on the slope, it was apparent that also **23** had a similar effect. To determine the IC₅₀ value, we obtained

Table 2. Second Series of Compounds and Their Biological Activity in HEK Cells

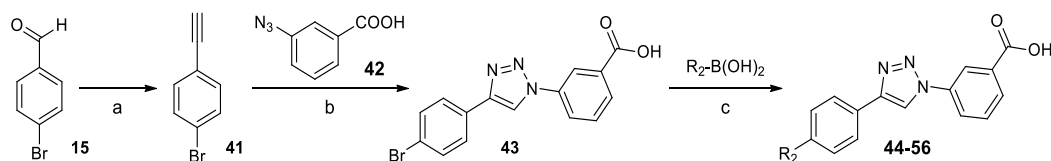
 series 2A					 series 2B			
R ₂	Cpd, Yield (%)	% SOCE inhibition (3 μM)	% Viability (10 μM)	IC ₅₀ (nM)	Cpd, Yield (%)	% SOCE inhibition (3 μM)	% Viability (10 μM)	IC ₅₀ (nM)
-	4, Synta66	86.7 ± 3.7	75.8 ± 8.0	228 ± 33				
	27, 55%	51.0 ± 31.9	-	-	44, 55%	1.8 ± 3.1	-	-
	28, 67%	45.9 ± 14.5	-	-	45, 22%	12.0 ± 18.9	-	-
	29, 86%	56.4 ± 21.0	-	-	46, 98%	53.0 ± 3.8	-	-
	30, 52%	25.8 ± 22.3	-	-	47, 46%	-22.8 ± 0.9	-	-
	31, 68%	85.1 ± 9.0	85.1 ± 1.9	807 ± 216	48, 61%	29.5 ± 22.7	-	-
	32, 18%	0.0 ± 13.1	-	-	-	-	-	-
	33, 80%	23.6 ± 33.7	-	-	49, 99%	0.0 ± 0.7	-	-
	34, 76%	96.5 ± 2.4	85.6 ± 1.3	851 ± 54	50, 76%	93.3 ± 5.1	93.1 ± 2.4	781 ± 37
	35, 76%	70.9 ± 7.9	90.5 ± 1.6	1621 ± 463	51, 91%	44.1 ± 17.1	-	-
	36, 86%	73.8 ± 11.3	94.3 ± 3.6	802 ± 160	52, 98%	75.4 ± 28.8	-	-
	37, 43%	54.3 ± 6.3	-	-	53, 56%	39.6 ± 7.6	-	-
	38, 75%	77.5 ± 8.2	93.5 ± 4.4	1198 ± 154	54, 99%	81.1 ± 7.0	71.7 ± 0.3	-
	39, 33%	67.3 ± 44.6	-	-	55, 58%	0.0 ± 4.29	-	-
	40, 46%	74.7 ± 6.3	91.1 ± 2.9	361 ± 42	56, 41%	88.9 ± 7.5	92.3 ± 3.1	866 ± 301

the concentration–response curves for both compounds (Figure 3C). **23** showed an IC₅₀ of 1.79 ± 0.14 μM, revealing approximately a 1 order of magnitude lower potency compared

to **Synta66** (IC₅₀ = 228 ± 33 nM). Moreover, **23** was slightly cytotoxic, with a residual cell viability of 71.8% at 10 μM, a characteristic shared by **Synta66** (75.8 ± 8.0%). To assess the

Scheme 3. Synthesis of Compounds 27–40 (Series 2A)^a

^aReagents and conditions: (a) NaNO_2 , NaN_3 , HCl , H_2O , rt, 5 h, 81%. (b) Sodium ascorbate, $\text{CuSO}_4 \cdot 5\text{H}_2\text{O}$, $t\text{-BuOH}$, H_2O , 50 °C, 48 h, 87%. (c) K_2CO_3 , $\text{Pd}(\text{OAc})_2$, EtOH , DMF , 80 °C, 6 h, 18–86%.

Scheme 4. Synthesis of Compounds 44–56 (Series 2B)^a

^aReagents and conditions: (a) Bestmann–Ohira reagent, K_2CO_3 , MeOH , rt, 18 h, 54%. (b) Sodium ascorbate, $\text{CuSO}_4 \cdot 5\text{H}_2\text{O}$, $t\text{-BuOH}$, H_2O , 50 °C, 16 h, 65%. (c) K_2CO_3 , $\text{Pd}(\text{OAc})_2$, EtOH , DMF , 80 °C, 6 h, 22–99%.

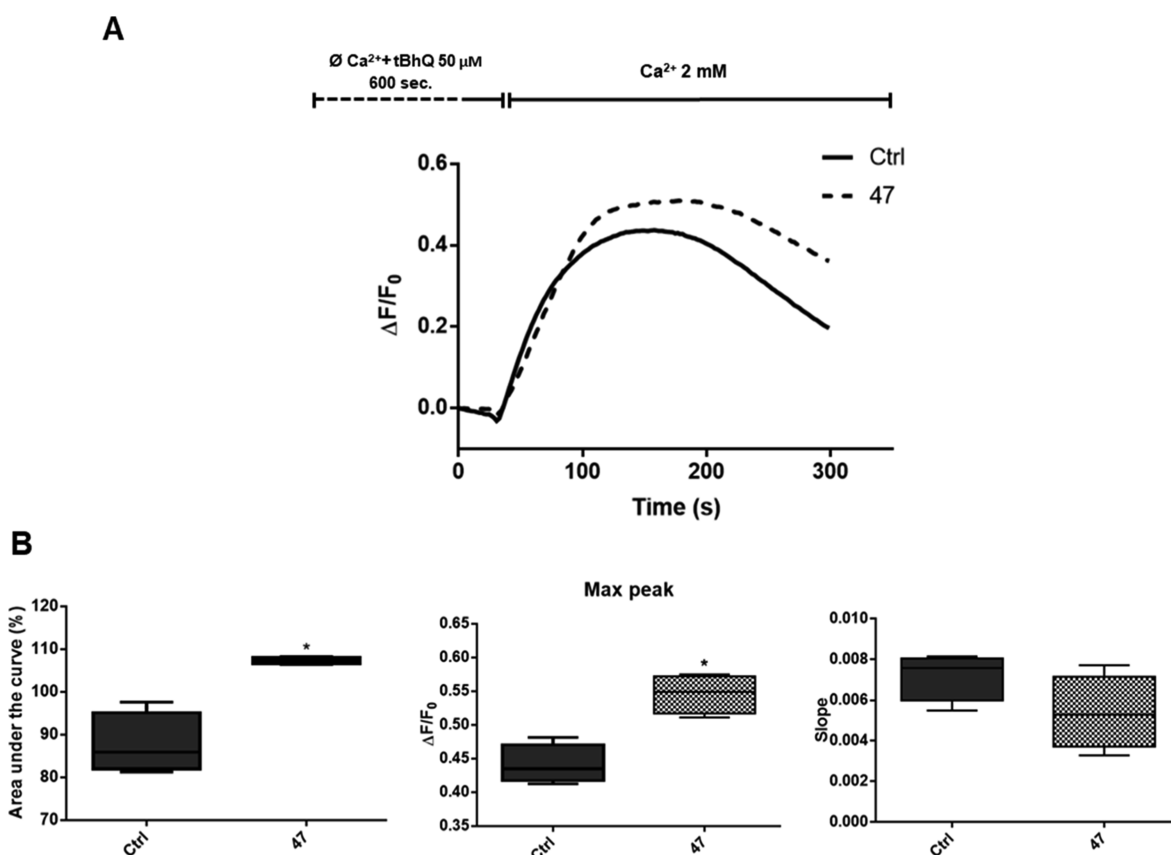


Figure 4. Effect of 47 on SOCE. (A) Average Ca^{2+} -traces of SOCE in the absence or presence of 47 ($3 \mu\text{M}$ in HEK cells). Traces are the average of 200 cells. (B) Evaluation of the AUC, peak amplitude, and slope of the Ca^{2+} -rise in the absence or presence of 47. The graph shows the median and IQR of the AUC, peak amplitude, and slope of the Ca^{2+} -rise. Mann–Whitney U test of compound *vs* control ($*p = 0.0286$).

cytotoxicity profile of the biphenyl triazoles, viability assays were performed on other molecules of the first series ($10 \mu\text{M}$) and all the compounds showed a cell viability comparable to 23 (data not shown).

SAR Study around 2,5-Dimethoxyphenyl Gives Compounds as Active as Synta66 on SOCE. The above data demonstrate that all the synthesized biphenyl triazoles showed a reduced activity on SOCE compared to Synta66. We therefore synthesized a second series of compounds (series 2A

and 2B, Figure 2) where the 2,5-dimethoxyphenyl ring, the only structural motif that had been kept fixed in our preliminary SAR, was extensively modified (Table 2). Given that the most potent compound in the first series featured a 3-carboxyphenyl ring, we decided to select this moiety as the one to keep fixed. The choice was also guided by the fact that this substructure was the preferred substitution in our previous paper reporting pyrtiazoles (CIC-37, Figure 1) and by the

perception that the 3-carboxyphenyl substrate is a privileged scaffold in SOCE modulation.¹⁶

To obtain the second series of biphenyl triazoles, a Suzuki cross-coupling reaction was exploited, starting from two aryl bromides, **26** and **43**, that were coupled with different boronic acids. **26** and **43** were synthesized as depicted in Schemes 3 and 4. Click chemistry reaction between azide **24**, prepared from 4-bromoaniline by diazotization-azidation protocol, and alkyne **25** afforded the aryl bromide **26**. Similarly, **43** was obtained by clicking alkyne **41**, synthesized by reacting 4-bromobenzaldehyde in the presence of the Bestmann–Ohira reagent, with azide **42**.

Starting from these two intermediates, 28 Suzuki reactions were performed and compounds **27–40** (series 2A, Figure 2) and **44–56** (series 2B, Figure 2) were synthesized. One reaction was instead not successful.

As described above, all the compounds were initially tested at 10 μM in HEK cells. This second series was significantly more potent compared to the first, and several molecules showed a noteworthy inhibitory activity, with percentage above 80% (data not shown). Therefore, in order to better discriminate between the different candidates, we decided to evaluate the effect of the compounds at 3 μM on SOCE. For those compounds that displayed SOCE inhibitory activity $\geq 70\%$, cell viability assays, this time at 10 μM , were then performed. For those molecules showing an inhibitory activity $\geq 70\%$ and a cell viability $\geq 85\%$, the IC_{50} values were calculated (Table 2).

The biological results highlighted that removal of both the methoxy substituents from positions 2' and 5' (**27**, $51.0 \pm 31.9\%$; **44**, $1.8 \pm 3.1\%$), or the presence of the solely 2'-methoxy substituent (**28**, $45.9 \pm 14.5\%$; **45**, $12.0 \pm 18.9\%$), caused a significant reduction of activity compared to Synta66 with a remarkable variability. On the other hand, the additional methoxy group at position 4' made the inhibition rise to 50% (**29**, $56.4 \pm 21.0\%$; **46**, $53.0 \pm 3.8\%$). When the same insertion was performed at position 6', for one compound a drop in inhibitory activity occurred (**30**, $25.8 \pm 22.3\%$), whereas for the other one (**47**) an increase in SOCE was surprisingly observed ($-22.8 \pm 0.9\%$, Figure 4A). The compound, tested at a concentration of 3 μM , significantly increased the AUC of calcium entry and the peak amplitude (Figure 4B), that is, represents a positive modulator of SOCE.

Given the absence of effect on slope, it is highly likely that it affects channel closure or desensitization. Given that the focus of this study was to identify novel SOCE negative modulators for the treatment of AP, the profile of compound **47** was not investigated further, but its discovery supports the idea that minor structural modifications of SOCE inhibitors can interfere with channel gating and produce activators, as already observed for pyrtiazoles (AL-2T (**57**), NM-3G (**58**); Figure 5)¹⁶ and for another recently described SOCE enhancer (IA65 (**59**), Figure 5).²² **47** therefore represents an enhancer of SOCE from a third distinct class of modulators and provides grounds to develop models to understand the mechanism by which this occurs.

Compound **31** in which the methoxy group is removed from position 2' while bearing a 3'-methoxy substituent was more active ($85.1 \pm 9.0\%$; Figure 6A) compared to Synta66, whereas the counterpart **48** was less active ($29.5 \pm 22.7\%$). The substitution of the methoxy group with a hydroxyl (**32**, $0.0 \pm 13.1\%$) or with a thioether (**33**, $23.6 \pm 33.7\%$; **49**, $0.0 \pm 0.7\%$) was instead not tolerated. Compounds **34** and **50** with a

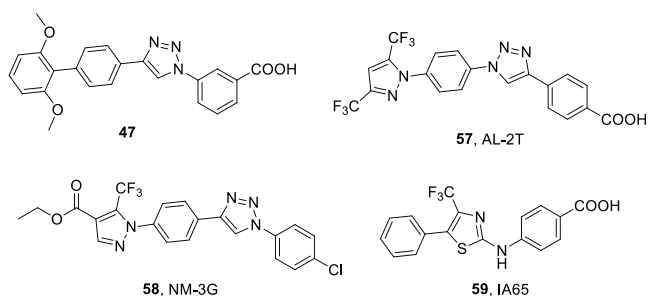


Figure 5. Structures of compound **47** and other positive modulators of SOCE reported in the literature.

2',3'-dimethoxy phenyl substituent also showed a good activity (96.5 ± 2.4 and $93.3 \pm 5.1\%$, respectively; Figure 6A), whereas if the two methoxy groups were fused together to form a 1,4-dioxanyl ring, the activity was lower (**35**, $70.9 \pm 7.9\%$ Figure 6A; **51**, $44.1 \pm 17.1\%$). The 3',5'-dimethoxy phenyl substituent provided a good inhibitory activity, as in the case of **36**, which induced an inhibition of $73.8 \pm 11.3\%$ (Figure 6A). On the other hand, **52** had a good inhibitory activity but due to its remarkable variability ($75.4 \pm 28.8\%$), the compound was not selected for further studies. The reduction of SOCE inhibition was also observed with the 3',4'-dimethoxy phenyl substituent but to a less extent (**37**, $54.3 \pm 6.3\%$; **53**, $39.6 \pm 7.6\%$). When the substituents in 3' and 4' were fused together in a six-member 1,4-dioxanyl ring, the activity rose (**38**, $77.5 \pm 8.2\%$, Figure 6A; **54**, $81.1 \pm 7.0\%$), whereas the 1,3-dioxolanyl was not tolerated in the case of **55** ($0.0 \pm 4.3\%$) and led to a less active compound with a high standard error in the case of **39** ($67.3 \pm 44.6\%$). Finally, a 2'-fluoro-5'-methoxy phenyl ring provided two compounds with remarkable activity on SOCE, **40** ($74.7 \pm 6.3\%$) and **56** ($88.9 \pm 7.5\%$), both reported in Figure 6A.

For all selected compounds (**31**, **34**, **35**, **36**, **38**, **40**, **50**, and **56**), the detailed analyses of the AUC, peak amplitude, and slope demonstrated that, similarly to Synta66, all compounds induced a drop in the three parameters, with **34** significantly reducing the AUC when compared to the reference compound. All these data are reported in the Supporting Information.

In summary, in the second series we were able to discover eight molecules with IC_{50} values in the nanomolar range (Figure 6B, Table 2).

Triazole is an Indispensable Feature of the New Class of Modulators and Reduces Off-Target Effects on DHODH. To better elucidate the role of the triazole ring in the interaction with SOCE machinery, we synthesized analogues of **38** displaying the direct (**64**) and the inverse (**69**) amides, according to Schemes 5 and 6. Suzuki cross-coupling reaction between (2,3-dihydrobenzo[*b*][1,4]dioxin-6-yl)boronic acid and 4-bromoaniline afforded amine **61** that, after coupling with 3-(methoxycarbonyl)benzoic acid and hydrolysis of the methyl ester, yielded compound **64**. (2,3-Dihydrobenzo[*b*][1,4]dioxin-6-yl)boronic acid and methyl 4-iodobenzoate underwent a Suzuki cross-coupling reaction and, after deprotection of the carboxylic group, afforded intermediate **66**. Then, **66** was coupled with methyl 3-aminobenzoate and the methyl ester hydrolyzed to give compound **69**.

The triazole ring is reputed to be a nonclassical bioisostere of amides,^{20,21} although we have shown in a number of

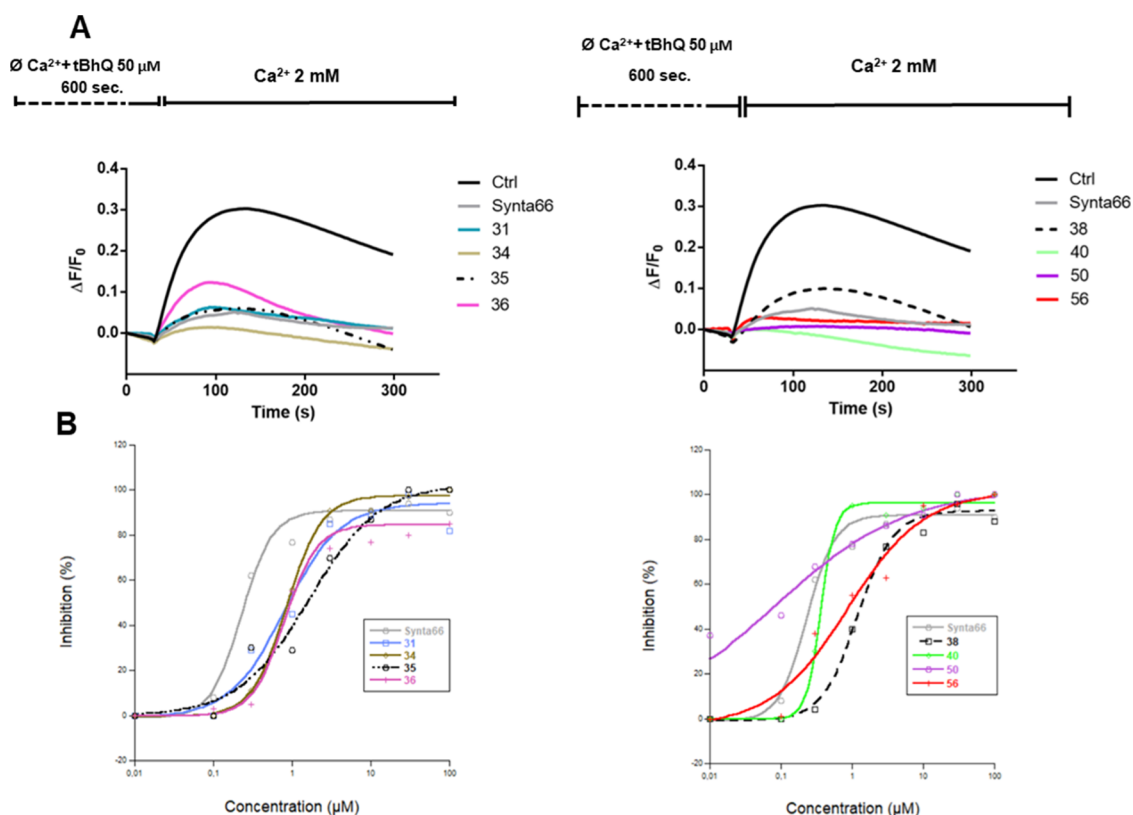
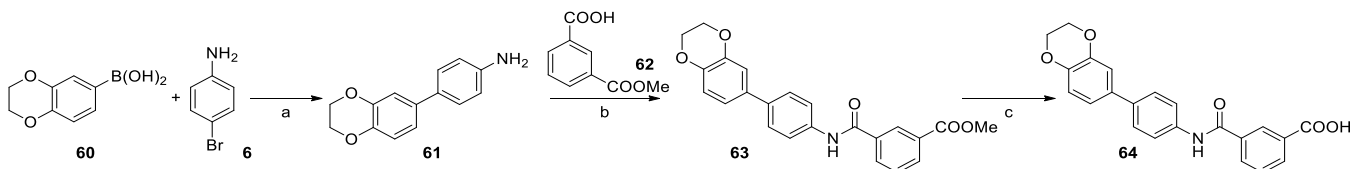


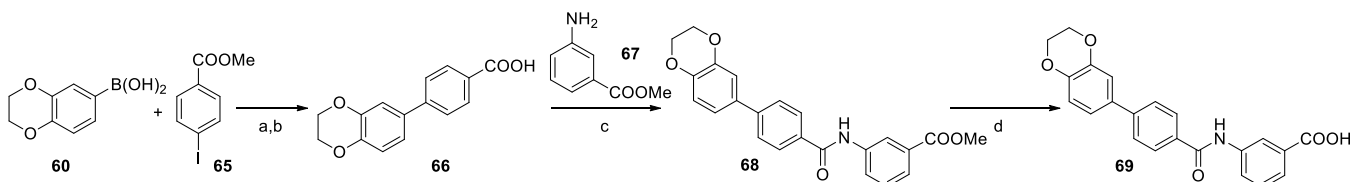
Figure 6. Effect of Synta66 and selected biphenyl triazoles on SOCE in HEK cells. (A) Average Ca^{2+} -traces of SOCE in the absence or presence of Synta66 or biphenyl triazoles (3 μM). Traces are the average of 200 cells. (B) Concentration–response curves.

Scheme 5. Synthesis of Compound 64^a



^aReagents and conditions: (a) K_2CO_3 , $\text{Pd}(\text{OAc})_2$, EtOH, DMF, 80 $^\circ\text{C}$, 6 h, 86%. (b) EDCl, DMAP, DIPEA, dry CH_2Cl_2 , rt, 18 h, 77%. (c) NaOH, H_2O , THF, 3 h, 60 $^\circ\text{C}$, 81%.

Scheme 6. Synthesis of Compound 69^a



^aReagents and conditions: (a) K_2CO_3 , $\text{Pd}(\text{OAc})_2$, EtOH, DMF, 80 $^\circ\text{C}$, 6 h. (b) NaOH, H_2O , THF, 4 h, 60 $^\circ\text{C}$, 85%. (c) EDCl, DMAP, DIPEA, dry CH_2Cl_2 , rt, 18 h, 63%. (d) NaOH, H_2O , THF, 4 h, 60 $^\circ\text{C}$, 61%.

occasions that this is not necessarily always the case.²³ To investigate the function of the triazole in this setting, we evaluated the amides of 38 (64 and 69). Both molecules displayed a significantly reduced activity compared to the parent compound (Table 3). It should be noticed that such a difference was also observed when comparing Synta66 with its triazole-substituted close analogues (9 and 18; Table 1).

Surprisingly, 64, despite its low activity on SOCE, showed a significant cytotoxicity, with a residual viability after 24 h of 50% at 10 μM in HEK cells, in contrast to its inverse amide 69

and 38, that did not affect cell viability. When attempting to rationalize this cytotoxicity, we noticed that 64 was structurally closely related to dihydroorotate dehydrogenase (DHODH) inhibitors.²⁴ Indeed, a *h*DHODH inhibitor usually includes a lipophilic moiety that guarantees the interaction with subsite 1 of the enzyme, together with a carboxylate moiety that interacts with the Arg136 residue located in subsite 2, two structural features that can be found in compound 64.

More surprisingly, a recent screening performed on an FDA database has highlighted that teriflunomide (70, Figure 7), a

Table 3. Amide Analogues of 38

Cpd,	X	% SOCE inhibition (3 μ M)	% Viability (10 μ M)	IC ₅₀
Yield (%)				
64, 81%		51.8 \pm 9.5	50.3 \pm 0.8	-
69, 61%		22.6 \pm 5.6	95.3 \pm 3.3	-

DHODH inhibitor approved for multiple sclerosis,²⁵ is endowed with a considerable inhibitory activity on SOCE (IC₅₀ = 4.3 \pm 1.0 μ M in HEK cells).²⁶ This led to asking whether **64** was a DHODH inhibitor and whether triazole-bearing analogues shared this feature. To investigate the involvement of DHODH, the cytotoxic activities of the two compounds bearing an amide substructure, **64** and **69**, and of the five selected biphenyl triazoles, **31**, **34**, **36**, **38**, **40**, were evaluated after 72 h at a high concentration (50 μ M) in HEK cells. Alongside, two well-characterized DHODH inhibitors, teriflunomide itself (**70**, Figure 7) and brequinar (**71**, Figure 7)²⁷ were used as reference compounds. Gratifyingly, the viability profile revealed that the biphenyl triazoles did not impair cell viability even at these high concentrations. For the arylamide-bearing molecules displaying a significant cytotoxicity (**64** and **Synta66**), the involvement of the *de novo* pyrimidine synthesis pathway was evaluated by supplementing the medium with an excess of uridine that should counterbalance the effect of DHODH inhibition by triggering the *de novo* pathway.²⁸ As expected, brequinar and teriflunomide were cytotoxic and their effect was reverted by uridine addition. The cytotoxic effect of **64** was also fully reverted by uridine, supporting our hypothesis that this is a DHODH inhibitor and that the substitution with the triazole ring reduces the off-target effects (Figure 7). While this observation deserves additional investigations, it questions whether other previously reported inhibitors bearing an aryl amide moiety might have promiscuous effects on this enzyme. Indeed, most SOCE inhibitors bear an amide-linkage as part of the pharmacophor-

e.^{15e} We preliminarily tested CM4620 and found that it was cytotoxic at 50 μ M in HEK cells but this cytotoxicity was not reverted by uridine, suggesting that it is not a DHODH inhibitor (not shown). A similar lack of effect was also observable for Pyr6, while no other arylamide SOCE inhibitor was tested.

Overall, these data corroborate previous evidence that the amide to triazole substitution is not merely bioisosteric (REF), as the presence of the triazole prevents off-target effects on DHODH.

Biphenyl Triazoles as Sodium Salts Are More Soluble Than Synta66. According to both potency and cell viability of the second series of modulators, the five most promising candidates were selected (**31**, **34**, **36**, **38**, and **40**), excluding those molecules that differed from these candidates only for the orientation of the triazole ring (**50** and **56**). To assess the druggability of the molecules, their thermodynamic aqueous solubility was evaluated. Unfortunately, the biphenyl triazoles showed poor aqueous solubility (about 0.20 μ g/mL, data not shown) comparable to that of **Synta66** (0.28 μ g/mL, Table 4). To overcome this limitation, the candidates were salified as sodium salts and their aqueous solubility was reassessed (Table 4). Briefly, except for **36**, all the tested biphenyl triazoles salts were soluble in water in the 0.67–1.53 mg/mL range. The presence of one or two methoxy substituents on the phenyl ring considerably increased the solubility compared to the 1,4-dioxanyl moiety of **38** as well as the addition of a fluorine atom that slightly improved the solubility of **40** compared to **31**. Interestingly, the enhanced solubility given by the methoxy substituents is minimally driven by the decrease in hydrophobicity but rather by the disruption of the molecular symmetry, as shown by the 80-fold increase in aqueous solubility of **34** compared to **36**. In addition, to assess the solubilization of the selected candidates in the aqueous vehicle used for *in vivo* administration, compounds **34** and **40** were dissolved at the nominal concentration of 6 mg/mL in saline solutions containing cosolvents (see methods section). Only **34** gave a limpid solution in saline containing 10% dimethyl sulfoxide (DMSO) + 20% PEG400, whose title was confirmed by LC–UV analysis, pointing to this compound as the best candidate for further *in vivo* evaluation.

Biphenyl Triazoles Are More Metabolically Stable Than Synta66. Next, the *in vitro* metabolic stability of the five candidates (**31**, **34**, **36**, **38**, and **40**) was evaluated in mouse

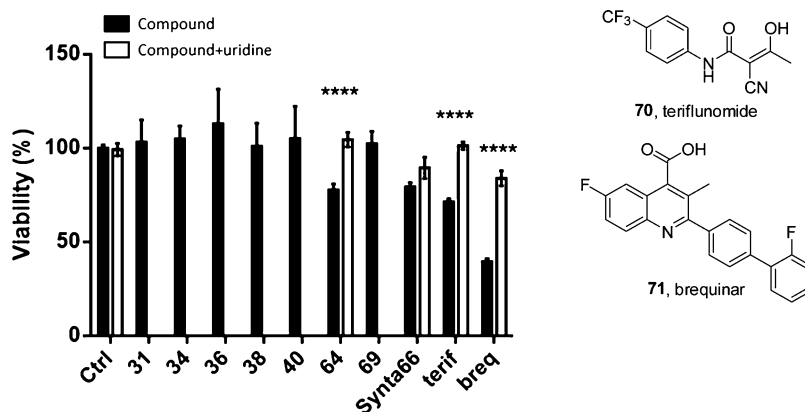
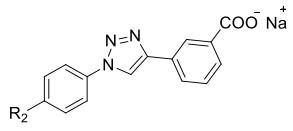
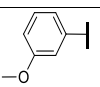
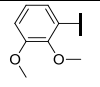
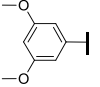
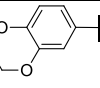
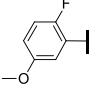


Figure 7. Effects of the selected compounds on DHODH. HEK cells were treated for 72 h at the concentration of 50 μ M with or without uridine (100 μ M). The graph shows average \pm SEM of cell viability, peak amplitude, and slope of the Ca²⁺-rise. A Student *t*-test was performed on compounds vs control (*****p* < 4.27 \times 10⁻⁶); (terif: teriflunomide, breq: brequinar).

Table 4. Aqueous Solubility and Metabolic Stability of the Selected Biphenyl Triazoles


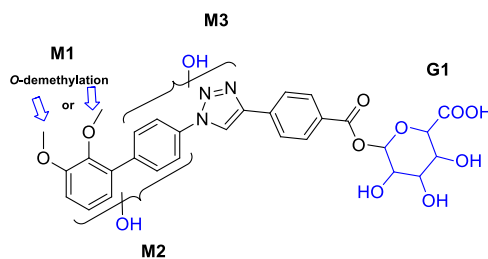
R ₂	Cpd	H ₂ O solubility (μg/mL)	Metabolic stability ^b
-	4, Synta66	0.28	15%
	31_Na	855.57	91%
	34_Na	1528.18 ^a	75%
	36_Na	18.72	92%
	38_Na	668.34	94%
	40_Na	1168.36	93%

^aSoluble at 6 mg/mL in saline containing 10% DMSO + 20% PEG400. ^bResidual substrate after 1 h incubation in MLMs.

liver microsomes (MLMs) activated by NADPH by measuring the substrate residual after 1 h. For comparative purposes, **Synta66** was incubated in the same conditions. All the salified biphenyl triazoles resulted in a quite stable microsomal oxidation, with a residual substrate in the range of 75–94% after incubation (Table 4). By contrast, **Synta66** resulted in a considerably less stable microsomal metabolism, with a substrate residual of only 15% after incubation, amide hydrolysis and *O*-demethylation metabolites showing the most extensive transformations (data not shown).

Next, the structural characterization of the metabolites of **34** was performed by high-resolution mass spectrometry (HRMS), processing the raw data with a workflow aimed at drug metabolite identification provided by Compound Discoverer 3.1 software (Thermo Scientific). Overall, data analysis highlighted the occurrence of three main transformations: *O*-demethylation (M1) followed by oxidation (M2) and hydroxylation (M3). Furthermore, incubation of **34** with MLMs in the presence of uridine diphosphate glucuronic acid (UDPGA) gave the corresponding acyl glucuronide metabolite G1 (Figure 8). Interestingly, data analysis did not highlight the formation of glutathione (GSH) adducts, suggesting that metabolism is not driven toward the formation of reactive species. Full data of metabolite structures and mass spectral data, as well as the metabolic pathways, are given in the Supporting Information.

34 Is Effective *In Vivo* in AP. To further characterize the compound, a PK analysis was performed in mice. Briefly, mice

**Figure 8.** Metabolic biotransformation of compound **34** in MLMs.

were injected with **34** (i.v., 7 mg/kg, once) and serial blood sampling was performed. **34** showed a half-life of 3.2 h, with a clearance of 0.5 L/h/kg, a volume of distribution of 2.3 L/kg, and a C_{\max} of 16.8 mg/L (see the Supporting Information for the full set of PK parameters).

The PK profile of our candidate prompted us to investigate its efficacy in a cerulein-induced murine model of AP.²⁹ The compound was administered 30 and 150 min after the first cerulein injection at a dose of 10 mg/kg i.p. The hematoxylin/eosin (H&E) staining of the pancreatic tissues collected 5 h after the first cerulein injection demonstrated that the compound was able to significantly ameliorate the histological scores, with reduction of inflammation and edema typical of this disease (Figure 9), as expected from SOCE inhibitors with profiles compatible with systemic administration.¹⁶

CONCLUSIONS

This work stems from our previous discovery that the pytriazole derivative **3**, originally designed from known pyrazole inhibitors, is an inhibitor of SOCE ($IC_{50} = 4.4 \mu\text{M} \pm 1.2$).¹⁶ The compound demonstrated efficacy in the cerulein-induced model of AP despite its short half-life (i.p., 1.3 h). With the aim of discovering drug-like SOCE inhibitors endowed with a better PK profile, the replacement of the amide with the triazole ring in **Synta66**, another well-known SOCE inhibitor extensively employed as chemical probe, was attempted.

The synthetic strategy relied on a two-step process based on a click chemistry reaction, followed by a Suzuki coupling. The performed SAR study highlighted that the pharmacophore of this novel class of modulators includes the phenyl ring bearing a methyl or methylene ether group in the meta position, the phenyl ring featuring a carboxylic group in the meta position, and the triazole ring. The latter, when switched into the direct or inverse amide, not only leads to a decrease in SOCE inhibition (**64** and **69**) but also to a significant cytotoxicity (**64**), which may in part be reconducted to the fact that arylamide substructures may act on DHODH. The summary of the SAR investigations is schematized in Figure 10.

Our efforts resulted in compound **34** that compared to **Synta66** (i) displays a slightly decreased potency on SOCE ($IC_{50} = 851 \pm 54 \text{ nM}$ vs $228 \pm 33 \text{ nM}$) but, importantly, no detectable cytotoxicity in HEK cells up to $60 \mu\text{M}$; (ii) shows a significantly higher *in vitro* metabolic stability in MLMs (75% vs 15% of residual substrate after 1 h); and (iii) is endowed with a carboxylic group that confers high aqueous solubility in the sodium salt form ($1528 \mu\text{g/mL}$ vs $0.28 \mu\text{g/mL}$). This yields a favorable PK profile in mice (i.v., $t_{1/2}$ of 3.2 h) and efficacy in a mouse model of cerulein-induced AP.

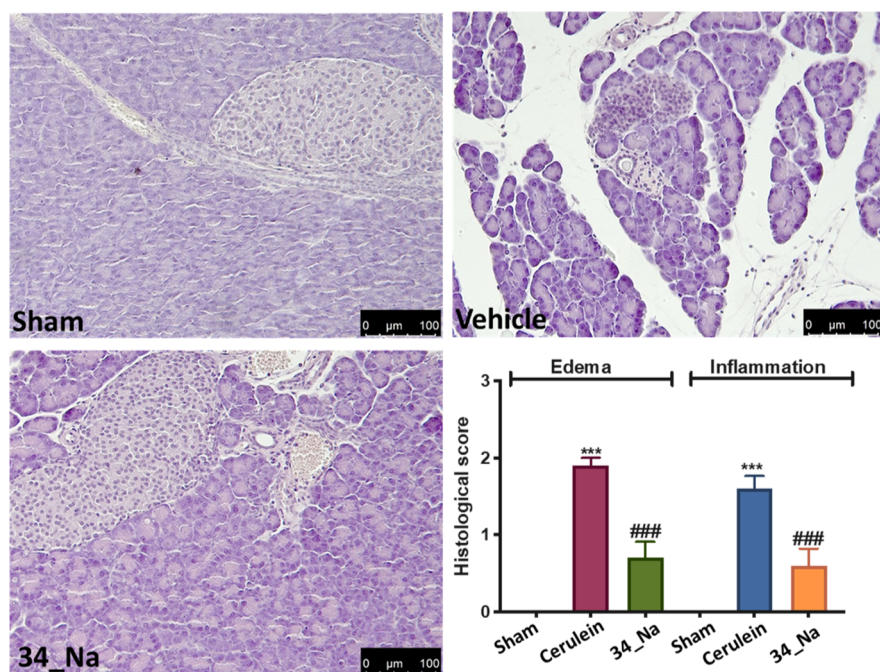


Figure 9. Evaluation of compound 34 in AP. H&E sections of pancreatic tissues. Analysis was performed in a blinded manner and data represent the mean \pm SEM of 10 mice for each group. *** $p < 0.001$ versus Sham; ### $p < 0.001$ vs cerulein.

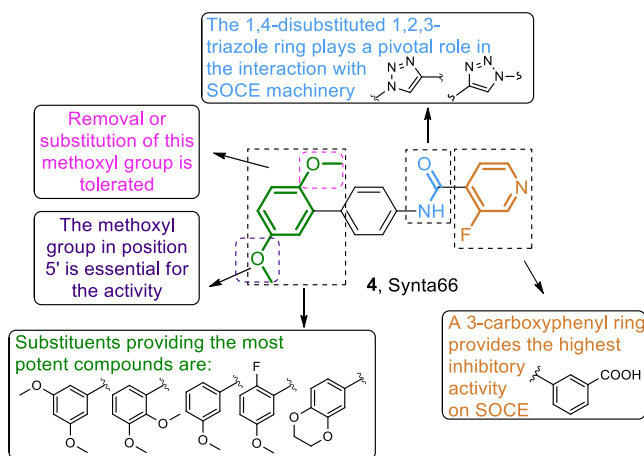


Figure 10. Graphical representation of SAR study around Synta66.

EXPERIMENTAL SECTION

Chemistry. General Experimental Methods. Reagents and solvents were used without further purification, although, if required, they were distilled and stored on molecular sieves. Column chromatography was performed on silica gel. The following instrumentation was used: Stuart scientific SMP3 apparatus (melting point), FT-IR Thermo-Nicolet Avatar, FT-IR Bruker Alpha II, Jeol ECP 300 MHz (^1H NMR), Bruker AVANCE Neo 400 MHz or Jeol ECP 300 MHz (^{13}C NMR), Thermo Finnigan LCQ-deca XP-plus equipped with an ESI source and an ion trap detector or mass spectrometry (Thermo Scientific Q-Exactive Plus) equipped with a heated electrospray ionization source. Chemical shifts are reported in parts per million (ppm). All lead compounds displayed a purity of 95% or higher, determined by HPLC (see the [Supporting Information](#)). Boronic acids, azides, and alkynes are commercially available or were synthesized following procedures reported in the literature, except for compounds 73, 75, 77, and 78 (intermediates for the synthesis of 18, 21, 9, and 13, respectively) that were synthesized as reported in the [Supporting Information](#).

2',5'-Dimethoxy-[1,1'-biphenyl]-4-amine, (7). 4-Bromoaniline (2 g, 11.63 mmol) was solubilized in DMF (23 mL) and ethanol (23 mL) under nitrogen atmosphere. 2,5-(Dimethoxyphenyl)boronic acid 5 (3.17 g, 17.44 mmol), $\text{Pd}(\text{OAc})_2$ (26.1 mg, 0.116 mmol), and K_2CO_3 (3.2 g, 23.26 mmol) were added in order. The mixture was stirred at 80 °C for 3 h and at room temperature overnight. The reaction was then filtered under vacuo over a pad of celite, rinsed with ethanol, and evaporated. The crude product was purified by column chromatography using petroleum ether/ethyl acetate 7:3 v/v as eluent, affording compound 7 as a yellow solid (2.61 g, 11.40 mmol, 98%); ^1H NMR (300 MHz, CDCl_3): δ 7.39 (d, $J = 6.9$ Hz, 2H), 6.97–6.88 (m, 2H), 6.84 (s, 1H), 6.70 (d, $J = 6.9$ Hz, 2H), 3.82 (s, 3H), 3.76 (s, 3H). MS (ESI) m/z : 230 $[\text{M} + \text{H}]^+$.

4'-Azido-2,5-dimethoxy-1,1'-biphenyl, (8). To a solution of 2',5'-dimethoxy-[1,1'-biphenyl]-4-amine (2 g, 8.73 mmol) in water (40 mL), HCl 37% (3.5 mL) was added dropwise and the resulting mixture was cooled down at 0 °C. Then, a solution of NaNO_2 (0.60 g, 8.73 mmol) in water (2 mL) was added and, after 10 min, a solution of NaN_3 (0.68 g, 10.48 mmol) in water (2 mL) was added dropwise. The reaction was stirred at room temperature for 5 h, diluted with ethyl acetate, and washed with water (2 \times). The organic layer was dried over sodium sulfate and the volatile was removed under vacuo. The crude material was purified by column chromatography using petroleum ether/ethyl acetate 98:2 v/v as eluent, yielding compound 8 as an orange solid (1.33 g, 5.24 mmol, 60%); ^1H NMR (300 MHz, CDCl_3): δ 8.31 (d, $J = 7.1$ Hz, 2H), 7.75 (d, $J = 7.1$ Hz, 2H), 6.92–6.83 (m, 3H), 3.85 (s, 3H), 3.79 (s, 3H).

General Procedure A. Compounds 9–14 were prepared from a suspension of 8 (74 mg, 0.29 mmol, 1 equiv) in water (320 μL) and *t*-BuOH (320 μL) and the relative alkyne (0.29 mmol, 1 equiv). Reactions were carried out overnight under vigorous stirring in the presence of sodium ascorbate 1 M (29 μL) and copper sulfate pentahydrate (0.0029 mmol, 0.01 equiv). Evaporation of the volatile and purification by silica gel column chromatography was performed.

4-(1-(2',5'-Dimethoxy-[1,1'-biphenyl]-4-yl)-1H-1,2,3-triazol-4-yl)-3-fluoropyridine, (9). Following general procedure A, the reaction of 8 and 4-ethynyl-3-fluoropyridine, after purification (petroleum ether/ethyl acetate 6:4 v/v as eluent), yielded 9 as a yellow solid (34 mg, 0.09 mmol, 31%); mp 165–166 °C. ^1H NMR (300 MHz, CDCl_3): δ 8.60–8.50 (m, 3H), 8.31 (d, $J = 6.1$ Hz, 1H), 7.85 (d, $J = 8.5$ Hz, 2H), 7.73 (d, $J = 8.5$ Hz, 2H), 6.97–6.89 (m, 3H), 3.83 (s,

3H), 3.75 (s, 3H). IR (KBr) $\bar{\nu}$: 3159, 3058, 2939, 1620, 1490, 1233, 1051, 842, 789 cm^{-1} . MS (ESI) m/z : 377 [M + H]⁺.

4-(1-(2',5'-Dimethoxy-[1,1'-biphenyl]-4-yl)-1H-1,2,3-triazol-4-yl)pyridine, (**10**). Following general procedure A, the reaction of **8** and 4-ethynylpyridine, after purification (petroleum ether/ethyl acetate 4:6 v/v as eluent), yielded compound **10** as a whitish solid (38 mg, 0.11 mmol, 37%); mp 185–186 °C. ¹H NMR (300 MHz, CDCl₃): δ 8.36 (s, 1H), 7.82 (d, J = 7.4 Hz, 2H), 7.73–7.64 (m, 4H), 7.52 (s, 1H), 6.97–6.90 (m, 4H), 3.82 (s, 3H), 3.80 (s, 3H). IR (KBr) $\bar{\nu}$: 3110, 2930, 2858, 1726, 1499, 1215, 821, 752, 727 cm^{-1} . MS (ESI) m/z : 359 [M + H]⁺.

3-(1-(2',5'-Dimethoxy-[1,1'-biphenyl]-4-yl)-1H-1,2,3-triazol-4-yl)pyridine, (**11**). Following general procedure A, the reaction of **8** and 3-ethynylpyridine, after purification (petroleum ether/ethyl acetate 5:5 v/v, petroleum ether/ethyl acetate 3:7 v/v and petroleum ether/ethyl acetate 2:8 v/v as eluents), yielded compound **11** as a yellow solid (68 mg, 0.19 mmol, 65%); mp 190–191 °C. ¹H NMR (300 MHz, CDCl₃): δ 9.11 (s, 1H), 8.63 (s, 1H), 8.31–8.29 (m, 2H), 7.83 (d, J = 8.3 Hz, 2H), 7.72 (d, J = 8.3 Hz, 2H), 7.43 (s, 1H), 6.97–6.91 (m, 3H), 3.94 (s, 3H), 3.79 (s, 3H). IR (KBr) $\bar{\nu}$: 3108, 2996, 2838, 1777, 1501, 1394, 1220, 806, 706 cm^{-1} . MS (ESI) m/z : 359 [M + H]⁺.

2-(1-(2',5'-Dimethoxy-[1,1'-biphenyl]-4-yl)-1H-1,2,3-triazol-4-yl)pyridine, (**12**). Following general procedure A, the reaction of **8** and 2-ethynylpyridine, after purification (petroleum ether/ethyl acetate 7:3 v/v as eluent), yielded compound **12** as a yellow solid (52 mg, 0.15 mmol, 50%); mp 166–167 °C. ¹H NMR (300 MHz, CDCl₃): δ 8.65–8.59 (m, 2H), 8.26 (d, J = 8.0 Hz, 1H), 7.85–7.78 (m, 3H), 7.70 (d, J = 8.5 Hz, 2H), 7.25 (t, J = 6.6 Hz, 1H), 6.95–6.86 (m, 3H), 3.82 (s, 3H), 3.77 (s, 3H). IR (KBr) $\bar{\nu}$: 3106, 2998, 2827, 1761, 1610, 1397, 1289, 810, 704 cm^{-1} . MS (ESI) m/z : 359 [M + H]⁺.

4-(1-(2',5'-Dimethoxy-[1,1'-biphenyl]-4-yl)-1H-1,2,3-triazol-4-yl)picolinic Acid, (**13**). Following general procedure A, the reaction of **8** and methyl 4-ethynylpicolinate, after purification (petroleum ether/ethyl acetate 4:6 v/v as eluent), yielded methyl 4-(1-(2',5'-dimethoxy-[1,1'-biphenyl]-4-yl)-1H-1,2,3-triazol-4-yl)picolinate as a yellow solid (39 mg, 0.09 mmol, 32%). The compound (39 mg, 0.09 mmol) was solubilized in acetone (390 μL) and water (390 μL). NaOH (7.2 mg, 0.18 mmol) was added and the mixture was stirred at room temperature for 1 h. The volatile was then removed and the crude material was purified by column chromatography using ethyl acetate/methanol 7:3 v/v as eluent, yielding compound **13** as a pale yellow solid (21 mg, 0.05 mmol, 58%); mp 162–163 °C. ¹H NMR (300 MHz, DMSO-*d*₆): δ 9.72 (s, 1H), 8.70–8.56 (m, 3H), 8.01 (d, J = 8.0 Hz, 2H), 7.75 (d, J = 8.0 Hz, 2H), 7.75 (s, 1H), 6.96 (m, 2H), 3.76 (s, 3H), 3.73 (s, 3H). IR (KBr) $\bar{\nu}$: 3158, 2932, 2858, 1726, 1499, 1225, 1075, 812, 758, 716 cm^{-1} . MS (ESI) m/z : 403 [M + H]⁺.

3-(1-(2',5'-Dimethoxy-[1,1'-biphenyl]-4-yl)-1H-1,2,3-triazol-4-yl)benzoic Acid, (**14**). Following general procedure A, the reaction of **8** and 3-ethynylbenzoic acid, after purification (petroleum ether/ethyl acetate 6:4 v/v as eluent), yielded compound **14** as a pale yellow solid (49 mg, 0.12 mmol, 42%); mp 177–178 °C. ¹H NMR (300 MHz, CDCl₃): δ 9.20 (s, 1H), 8.66 (s, 1H), 8.28 (d, J = 8.0 Hz, 1H), 8.04 (d, J = 6.6 Hz, 2H), 7.73 (d, J = 6.6 Hz, 2H), 7.67–7.53 (m, 2H), 7.08 (d, J = 8.0 Hz, 1H), 7.01–6.92 (m, 2H), 3.82 (s, 3H), 3.79 (s, 3H). IR (KBr) $\bar{\nu}$: 3155, 2961, 1727, 1497, 1263, 1217, 1073, 810, 756 cm^{-1} . MS (ESI) m/z : 402 [M + H]⁺.

2',5'-Dimethoxy-[1,1'-biphenyl]-4-carbaldehyde, (**16**). To a solution of 4-bromobenzaldehyde **15** (500 mg, 2.70 mmol) in DMF (8 mL) and water (2 mL) (2,5-dimethoxyphenyl)boronic acid **5** (540 mg, 2.97 mmol), Pd(OAc)₂ (11.2 mg, 0.05 mmol) and K₂CO₃ (933 mg, 6.75 mmol) were added in order under nitrogen atmosphere and stirred at 50 °C for 3 h. The reaction was filtered under vacuo over a pad of celite, diluted with diethyl ether, and washed three times with water. The organic phase was dried over sodium sulfate and evaporated. Purification by column chromatography (petroleum ether/ethyl acetate 98:2 v/v) yielded compound **16** as an orange solid (647 mg, 2.67 mmol, 99%). ¹H NMR (300 MHz, CDCl₃): δ 10.06 (s, 1H), 7.89 (d, J = 7.7 Hz, 2H), 7.69 (d, J = 7.7 Hz, 2H),

7.08–6.91 (m, 3H), 3.79 (s, 3H), 3.73 (s, 3H). MS (ESI) m/z : 243 [M + H]⁺.

4'-Ethynyl-2,5-dimethoxy-1,1'-biphenyl, (**17**). To a solution of intermediate **16** (636 mg, 2.63 mmol) in MeOH (6 mL), K₂CO₃ (727 mg, 5.26 mmol) and dimethyl (1-diazo-2-oxopropyl)phosphonate (759 mg, 3.95 mmol) were added in order under nitrogen atmosphere. The mixture was stirred at room temperature overnight, then the solvent was removed, water was added, and the aqueous layer was extracted with CH₂Cl₂ (3 \times). The organic phases were collected, dried over sodium sulfate, and evaporated. Purification by column chromatography (petroleum ether/ethyl acetate 98:2 v/v as eluent) yielded compound **17** as a white solid (514 mg, 2.16 mmol, 82%). ¹H NMR (300 MHz, CDCl₃): δ 7.59–7.49 (m, 4H), 6.93–6.85 (m, 3H), 3.86 (s, 3H), 3.76 (s, 3H), 3.10 (s, 1H). MS (ESI) m/z : 239 [M + H]⁺.

General Procedure B. Compounds **18**–**23** were prepared from a suspension of **17** (0.29 mmol, 1 equiv) in water (320 μL) and *t*-BuOH (320 μL) and the relative azide (0.29 mmol, 1 equiv). Reactions were carried out overnight under vigorous stirring in the presence of sodium ascorbate 1 M (30 μL) and copper sulfate pentahydrate (0.0029 mmol, 0.01 equiv). Evaporation of the volatile and purification by silica gel column chromatography was performed.

4-(4-(2',5'-Dimethoxy-[1,1'-biphenyl]-4-yl)-1H-1,2,3-triazol-1-yl)-3-fluoropyridine, (**18**). Following general procedure B, the reaction of **17** and 4-azido-3-fluoropyridine, after purification (petroleum ether/ethyl acetate 7:3 v/v as eluent), yielded compound **18** as a yellow solid (95 mg, 0.25 mmol, 60%); mp 176–177 °C. ¹H NMR (300 MHz, CDCl₃): δ 8.75 (s, 1H), 8.64 (d, J = 6.0 Hz, 1H), 8.48 (s, 1H), 8.22 (d, J = 6.0 Hz, 1H), 7.96 (d, J = 8.3 Hz, 2H), 7.66 (d, J = 8.3 Hz, 2H), 6.96–6.89 (m, 3H), 3.82 (s, 3H), 3.76 (s, 3H). IR (KBr) $\bar{\nu}$: 3135, 3002, 2837, 1735, 1488, 1216, 1022, 828, 805, 714 cm^{-1} . MS (ESI) m/z : 377 [M + H]⁺.

4-(4-(2',5'-Dimethoxy-[1,1'-biphenyl]-4-yl)-1H-1,2,3-triazol-1-yl)pyridine, (**19**). Following general procedure B, the reaction of **17** and 4-azidopyridine, after purification (petroleum ether/ethyl acetate 9:1 v/v as eluent), yielded compound **19** as a yellow solid (119 mg, 0.33 mmol, 79%); mp 179–180 °C. ¹H NMR (300 MHz, DMSO-*d*₆): δ 9.55 (s, 1H), 8.85 (s, 1H), 8.04–8.01 (m, 2H), 7.99 (d, J = 8.3 Hz, 2H), 7.66 (d, J = 8.3 Hz, 2H), 7.06 (d, J = 6.9 Hz, 1H), 6.94–6.93 (m, 3H), 3.77 (s, 3H), 3.74 (s, 3H). IR (KBr) $\bar{\nu}$: 3109, 2961, 2837, 1498, 1488, 1396, 1261, 819, 805, 753 cm^{-1} . MS (ESI) m/z : 359 [M + H]⁺.

3-(4-(2',5'-Dimethoxy-[1,1'-biphenyl]-4-yl)-1H-1,2,3-triazol-1-yl)pyridine, (**20**). Following general procedure B, the reaction of **17** and 3-azidopyridine, after purification (petroleum ether/ethyl acetate 5:5 v/v as eluent), yielded compound **20** as a yellowish solid (117 mg, 0.33 mmol, 78%); mp 184–185 °C. ¹H NMR (300 MHz, CDCl₃): δ 9.08 (s, 1H), 8.72 (s, 1H), 8.27–8.21 (m, 2H), 7.95 (d, J = 8.3 Hz, 2H), 7.65 (d, J = 8.3 Hz, 2H), 7.53 (t, J = 5.2 Hz, 1H), 6.96–6.88 (m, 3H), 3.82 (s, 3H), 3.78 (s, 3H). IR (KBr) $\bar{\nu}$: 3108, 2963, 2837, 1585, 1485, 1261, 1025, 820, 805, 700 cm^{-1} . MS (ESI) m/z : 359 [M + H]⁺.

Methyl 4-(4-(2',5'-Dimethoxy-[1,1'-biphenyl]-4-yl)-1H-1,2,3-triazol-1-yl)picolinate, (**21**). Following general procedure B, the reaction of **17** and methyl 4-azidopicolinate, after purification (petroleum ether/ethyl acetate 4:6 v/v as eluent), yielded compound **21** as a yellowish solid (107 mg, 0.26 mmol, 61%); mp 145.5–146.5 °C. ¹H NMR (300 MHz, (CD₃)₂CO): δ 9.38 (s, 1H), 8.93 (d, J = 4.6 Hz, 1H), 8.65 (s, 1H), 8.26 (d, J = 9.0 Hz, 1H), 8.05 (d, J = 8.3 Hz, 2H), 7.67 (d, J = 8.3 Hz, 2H), 7.05 (d, J = 9.0 Hz, 1H), 6.95–6.91 (m, 2H), 4.03 (s, 3H), 3.81 (s, 3H), 3.77 (s, 3H). IR (KBr) $\bar{\nu}$: 3160, 2928, 2840, 1760, 1495, 1466, 1306, 1259, 1200, 828, 732 cm^{-1} . MS (ESI) m/z : 417 [M + H]⁺.

4-(4-(2',5'-Dimethoxy-[1,1'-biphenyl]-4-yl)-1H-1,2,3-triazol-1-yl)picolinic Acid, (**22**). Compound **21** (49 mg, 0.12 mmol) was solubilized in acetone (490 μL) and water (490 μL). NaOH (9.6 mg, 0.24 mmol) was added and the mixture was stirred at room temperature for 2 h. Evaporation of the volatile and purification by column chromatography (ethyl acetate/methanol 8:2 v/v and ethyl acetate/methanol 7:3 v/v as eluents) yielded compound **22** as a pale yellow solid (36 mg, 0.09 mmol, 75%); mp 158–159 °C. ¹H NMR (300 MHz, DMSO-*d*₆): δ 9.71 (s, 1H), 8.70–8.62 (m, 3H), 8.02 (d, J

= 8.0 Hz, 2H), 7.63 (d, J = 8.0 Hz, 2H), 7.09 (d, J = 9.6 Hz, 1H), 6.94–6.92 (m, 2H), 3.80 (s, 3H), 3.76 (s, 3H). IR (KBr) $\bar{\nu}$: 3159, 2931, 2856, 1706, 1490, 1485, 1308, 1260, 1206, 830, 742 cm^{-1} . MS (ESI) m/z : 403 $[\text{M} + \text{H}]^+$.

3-(4-(2',5'-Dimethoxy-[1,1'-biphenyl]-4-yl)-1H-1,2,3-triazol-1-yl)-benzoic Acid, (23). Following general procedure B, the reaction of 17 and 3-azidobenzoic acid, after purification (petroleum ether/ethyl acetate 3:7 v/v as eluent), yielded compound 23 as a yellowish solid (167 mg, 0.42 mmol, 99%); mp 215–216 °C. ^1H NMR (300 MHz, CDCl_3): δ 9.18 (s, 1H), 8.58 (s, 1H), 8.26 (d, J = 8.0 Hz, 1H), 8.15 (d, J = 8.0 Hz, 1H), 8.05 (d, J = 6.9 Hz, 2H), 7.77 (t, J = 8.0 Hz, 1H), 7.65 (d, J = 6.9 Hz, 2H), 7.04 (d, J = 9.0 Hz, 1H), 6.97–6.89 (m, 2H), 3.80 (s, 3H), 3.76 (s, 3H). ^{13}C NMR (101 MHz, $\text{DMSO}-d_6$): δ 166.9, 153.9, 150.8, 147.9, 138.4, 137.3, 133.5, 130.9, 130.6, 130.3, 129.7, 129.2, 125.5, 124.3, 120.8, 120.2, 116.4, 114.1, 113.7, 56.7, 56.0. IR (KBr) $\bar{\nu}$: 3159, 2931, 1711, 1495, 1312, 1243, 1210, 839, 753 cm^{-1} . MS (ESI) m/z : 402 $[\text{M} + \text{H}]^+$.

1-Azido-4-bromobenzene, (24). To a solution of 4-bromoaniline (3 g, 17.44 mmol) in water (77 mL) HCl 37% (7 mL) was added dropwise and the resulting mixture was cooled down at 0 °C. Then, a solution of NaNO_2 (1.20 g, 17.44 mmol) in water (3 mL) was added and, after 10 min, a solution of NaN_3 (1.36 g, 20.92 mmol) in water (3 mL) was added dropwise. The reaction was stirred at room temperature for 3 h, diluted with ethyl acetate, and washed with water (2X). The organic layer was dried over sodium sulfate and the volatile was removed under vacuo. Purification by column chromatography (petroleum ether/ethyl acetate 98:2 v/v as eluent) yielded compound 24 as an orange solid (4.86 g, 14.13 mmol, 81%); ^1H NMR (300 MHz, CDCl_3): δ 7.53–7.44 (m, 2H), 6.97–6.88 (m, 2H).

3-(1-(4-Bromophenyl)-1H-1,2,3-triazol-4-yl)benzoic Acid, (26). To a suspension of 1-azido-4-bromobenzene 24 (2.78 g, 14.04 mmol) in water (26 mL) and *t*-BuOH (26 mL) 3-ethynylbenzoic acid 25 (2.05 g, 14.04 mmol) was added. Then, 1.4 mL of an aqueous solution of sodium ascorbate 1 M and copper sulfate pentahydrate (34.9 mg, 0.14 mmol) were added and the mixture was vigorously stirred for 48 h. Evaporation and purification by column chromatography (petroleum ether/ethyl acetate 2:8 v/v and ethyl acetate/methanol 8:2 v/v as eluents) yielded compound 26 as a yellow solid (4.22 g, 12.27 mmol, 87%); ^1H NMR (300 MHz, $\text{DMSO}-d_6$): δ 9.54 (s, 1H), 8.51 (s, 1H), 8.14 (d, J = 7.7 Hz, 1H), 7.98–7.94 (m, 3H), 7.86–7.83 (d, J = 8.8 Hz, 2H), 7.60 (t, J = 7.7 Hz, 1H). MS (ESI) m/z : 343 $[\text{M} - \text{H}]^-$.

General Procedure C. Compounds 27–40 were prepared from a solution of 26 (0.29 mmol, 1 equiv) in DMF (750 μL) and ethanol (750 μL) under nitrogen atmosphere in the presence of the relative boronic acid (0.44 mmol, 1.5 equiv). Reactions were carried out at 80 °C overnight in the presence of $\text{Pd}(\text{OAc})_2$ (0.0029 mmol, 0.01 equiv) and K_2CO_3 (0.58 mmol, 2 equiv). After filtration of the reaction mixture under vacuo over a pad of celite and evaporation of the volatile, purification by silica gel column chromatography was performed.

3-(1-([1,1'-Biphenyl]-4-yl)-1H-1,2,3-triazol-4-yl)benzoic Acid, (27). Following general procedure C, the reaction of 26 and phenylboronic acid, after purification (petroleum ether/ethyl acetate 4:6 v/v as eluent), yielded compound 27 as a yellow solid (54.5 mg, 0.16 mmol, 55%); mp 232–234 °C dec. ^1H NMR (300 MHz, $\text{DMSO}-d_6$): δ 9.52 (s, 1H), 8.61 (s, 1H), 8.20 (d, J = 6.9 Hz, 1H), 8.09 (d, J = 8.3 Hz, 2H), 7.98–7.85 (m, 3H), 7.77 (d, J = 8.3 Hz, 2H), 7.63 (t, J = 7.5 Hz, 1H), 7.54–7.50 (m, 2H), 7.43 (d, J = 7.5 Hz, 1H). ^{13}C NMR (101 MHz, $\text{DMSO}-d_6$): δ 167.7, 147.1, 140.9, 139.3, 136.3, 134.5, 132.4, 131.1, 129.8, 129.5, 129.4, 128.5, 128.5, 127.2, 126.6, 120.9, 120.5. IR (neat) $\bar{\nu}$: 2922, 2852, 1719, 1687, 1525, 1489, 1299, 1227, 1154, 814, 158, 682 cm^{-1} . MS (ESI) m/z : 342 $[\text{M} + \text{H}]^+$. HRMS (ESI) m/z : $(\text{M} + \text{H})^+$ calcd for $\text{C}_{21}\text{H}_{16}\text{N}_3\text{O}_2$, 342.1237; found, 342.1234.

3-(1-(2'-Methoxy-[1,1'-biphenyl]-4-yl)-1H-1,2,3-triazol-4-yl)-benzoic Acid, (28). Following general procedure C, the reaction of 26 and (2-methoxyphenyl)boronic acid, after purification (ethyl acetate as eluent), yielded compound 28 as a yellow solid (72 mg, 0.19 mmol, 67%); mp 208–209 °C. ^1H NMR (300 MHz, $\text{DMSO}-d_6$): δ 9.45 (s,

1H), 8.56 (s, 1H), 8.18 (d, J = 6.9 Hz, 1H), 8.03–7.95 (m, 3H), 7.74 (d, J = 8.3 Hz, 2H), 7.53 (t, J = 6.9 Hz, 1H), (d, J = 8.3 Hz, 2H), 7.24–7.14 (m, 2H), 3.82 (s, 3H). ^{13}C NMR (101 MHz; $\text{DMSO}-d_6$): δ 167.9, 156.6, 147.1, 139.0, 135.7, 133.3, 131.1, 130.8, 129.9, 129.8, 129.5, 128.9, 126.6, 122.3, 121.4, 120.6, 120.5, 120.1, 112.3, 56.0. IR (neat) $\bar{\nu}$: 3127, 2923, 2851, 1718, 1685, 1595, 1487, 1227, 1024, 756, 745 cm^{-1} . MS (ESI) m/z : 372 $[\text{M} + \text{H}]^+$. HRMS (ESI) m/z : $(\text{M} + \text{H})^+$ calcd for $\text{C}_{22}\text{H}_{18}\text{N}_3\text{O}_3$, 372.1343; found, 372.1337.

3-(1-(2',4'-Dimethoxy-[1,1'-biphenyl]-4-yl)-1H-1,2,3-triazol-4-yl)-benzoic Acid, (29). Following general procedure C, the reaction of 26 and (2,4-dimethoxyphenyl)boronic acid, after purification (ethyl acetate/methanol 9:1 v/v as eluent), yielded compound 29 as a pale yellow solid (100 mg, 0.25 mmol, 86%); mp 235–236 °C. ^1H NMR (300 MHz, $\text{DMSO}-d_6$): δ 9.47 (s, 1H), 8.56 (s, 1H), 8.17 (d, J = 8.2 Hz, 1H), 7.99–7.95 (m, 3H), 7.69 (d, J = 9.2 Hz, 2H), 7.62 (t, J = 8.2 Hz, 1H), 7.32 (d, J = 8.2 Hz, 1H), 6.71 (s, 1H), 6.66 (d, J = 6.2 Hz, 1H), 3.83 (s, 3H), 3.81 (s, 3H). ^{13}C NMR (75 MHz; $\text{DMSO}-d_6$): δ 168.2, 161.1, 157.8, 147.2, 139.1, 135.4, 133.4, 131.5, 131.1, 130.9, 129.7, 129.6, 129.5, 126.6, 121.6, 120.5, 120.1, 106.1, 99.6, 56.2, 55.9. IR (neat) $\bar{\nu}$: 3406, 3020, 2929, 1687, 1605, 1499, 1414, 1279, 1161, 1026, 803, 761 cm^{-1} . MS (ESI) m/z : 402 $[\text{M} + \text{H}]^+$. HRMS (ESI) m/z : $(\text{M} + \text{H})^+$ calcd for $\text{C}_{23}\text{H}_{20}\text{N}_3\text{O}_4$, 402.1448; found, 402.1441.

3-(1-(2',6'-Dimethoxy-[1,1'-biphenyl]-4-yl)-1H-1,2,3-triazol-4-yl)-benzoic Acid, (30). Following general procedure C, the reaction of 26 and (2,6-dimethoxyphenyl)boronic acid, after purification (ethyl acetate/methanol 9:1 v/v as eluent), yielded compound 30 as a pale yellow solid (60 mg, 0.15 mmol, 52%); mp 248–250 °C dec. ^1H NMR (300 MHz, $\text{DMSO}-d_6$): δ 9.40 (s, 1H), 8.55 (s, 1H), 8.15 (d, J = 6.9 Hz, 1H), 7.97–7.95 (m, 4H), 7.84 (d, J = 6.9 Hz, 1H), 7.62–7.58 (m, 1H), 7.47 (d, J = 8.2 Hz, 1H), 7.35 (t, J = 8.2 Hz, 1H), 6.79 (d, J = 8.2 Hz, 1H), 3.71 (s, 6H). ^{13}C NMR (101 MHz; $\text{DMSO}-d_6$): δ 168.3, 157.6, 147.4, 147.1, 135.5, 135.3, 133.3, 132.7, 130.4, 129.6, 129.3, 126.6, 122.4, 120.5, 119.9, 117.8, 105.0, 56.3. IR (neat) $\bar{\nu}$: 3409, 2923, 2834, 1701, 1591, 1400, 1246, 1100, 825, 756 cm^{-1} . MS (ESI) m/z : 402 $[\text{M} + \text{H}]^+$. HRMS (ESI) m/z : $(\text{M} + \text{H})^+$ calcd for $\text{C}_{23}\text{H}_{20}\text{N}_3\text{O}_4$, 402.1448; found, 402.1441.

3-(1-(3'-Methoxy-[1,1'-biphenyl]-4-yl)-1H-1,2,3-triazol-4-yl)-benzoic Acid, (31). Following general procedure C, the reaction of 26 and (3-methoxyphenyl)boronic acid, after purification (ethyl acetate/methanol 9:1 v/v as eluent), yielded compound 31 as a white solid (73 mg, 0.20 mmol, 68%); mp 244–245 °C. ^1H NMR (400 MHz, $\text{DMSO}-d_6$): 9.57 (s, 1H), 8.56 (s, 1H), 8.23 (d, J = 7.4 Hz, 1H), 8.09 (d, J = 8.2 Hz, 2H), 7.96–7.94 (m, 3H), 7.65 (t, J = 7.6 Hz, 1H), 7.43 (t, J = 7.6 Hz, 1H), 7.33 (d, J = 7.6 Hz, 1H), 7.30 (s, 1H), 6.99 (d, J = 7.4 Hz, 1H), 3.86 (s, 3H). ^{13}C NMR (101 MHz; $\text{DMSO}-d_6$): δ 167.5, 160.3, 147.1, 140.7 (2C), 136.3, 132.2, 131.1, 130.6, 129.9, 129.8, 129.4, 128.7, 126.5, 120.7, 120.6, 119.5, 114.1, 112.7, 55.7. IR (KBr) $\bar{\nu}$: 3450, 2837, 1909, 1513, 1244, 1033, 801, 677 cm^{-1} . MS (ESI) m/z : 372 $[\text{M} + \text{H}]^+$. For biological evaluation, the sodium salt of 31 was prepared by dissolving it in THF and adding a 50% aqueous solution of NaOH (1 equiv). After stirring at 60 °C for 1 h, the solid precipitate was collected by filtration; mp 182–183 °C dec.

3-(1-(3'-Hydroxy-[1,1'-biphenyl]-4-yl)-1H-1,2,3-triazol-4-yl)-benzoic Acid, (32). Following general procedure C, the reaction of 26 and (3-hydroxyphenyl)boronic acid, after purification (ethyl acetate/methanol 9:1 v/v and ethyl acetate/methanol 8:2 v/v as eluents), yielded compound 32 as a dark yellow solid (19 mg, 0.05 mmol, 18%); mp 184–186 °C dec. ^1H NMR (300 MHz, CD_3OD): δ 8.96 (s, 1H), 8.59 (s, 1H), 8.15 (s, 1H), 8.03 (d, J = 7.8 Hz, 1H), 7.92 (d, J = 7.4 Hz, 1H), 7.58 (d, J = 7.8 Hz, 1H), 7.18–7.15 (m, 3H), 7.04–6.99 (m, 2H), 6.82 (d, J = 5.8 Hz, 2H). ^{13}C NMR (101 MHz, $\text{DMSO}-d_6$): δ 168.2, 157.0, 133.3, 130.9, 130.6, 130.4, 129.6, 129.4, 129.4, 129.2, 128.8, 128.4, 126.6, 125.2, 122.4, 121.3, 120.8, 120.5, 117.4. IR (neat) $\bar{\nu}$: 3406, 2924, 1686, 1613, 1303, 1229, 1034, 887, 757, 700, 683 cm^{-1} . MS (ESI) m/z : 356 $[\text{M}-\text{H}]^-$. HRMS (ESI) m/z : $(\text{M} + \text{H})^+$ calcd for $\text{C}_{21}\text{H}_{16}\text{N}_3\text{O}_3$, 358.1186; found, 358.1180.

3-(1-(3'-(Methylthio)-[1,1'-biphenyl]-4-yl)-1H-1,2,3-triazol-4-yl)-benzoic Acid, (33). Following general procedure C, the reaction of 26 and (3-(methylthio)phenyl)boronic acid, after purification (ethyl acetate/methanol 9:1 v/v as eluent), yielded compound 33 as a white

solid (89.8 mg, 0.23 mmol, 80%); mp 258–259 °C. ¹H NMR (300 MHz, DMSO-*d*₆): δ 9.55 (s, 1H), 8.55 (s, 1H), 8.18 (d, *J* = 7.9 Hz, 1H), 8.08 (d, *J* = 9.3 Hz, 2H), 7.97–7.95 (m, 3H), 7.60 (d, *J* = 9.3 Hz, 2H), 7.52 (d, *J* = 7.9 Hz, 1H), 7.45 (t, *J* = 7.9 Hz, 1H), 7.31 (d, *J* = 6.2 Hz, 1H), 2.58 (s, 3H). ¹³C NMR (75 MHz; DMSO-*d*₆): δ 168.1, 147.3, 140.5, 140.1, 139.8, 136.5, 133.1, 131.1, 130.5, 130.1, 129.8, 129.7, 129.5, 128.8, 126.6, 125.9, 124.5, 123.9, 120.8, 15.2. IR (KBr) $\bar{\nu}$: 3450, 3127, 2917, 1521, 1305, 1229, 1043, 838, 696 cm⁻¹. MS (ESI) *m/z*: 388 [M + H]⁺. HRMS (ESI) *m/z*: (M + H)⁺ calcd for C₂₂H₁₈N₃O₃S, 388.1114; found, 388.1107.

3-(1-(2',3'-Dimethoxy-[1,1'-biphenyl]-4-yl)-1H-1,2,3-triazol-4-yl)-benzoic Acid, (34). Following general procedure C, the reaction of **26** and (2,3-dimethoxyphenyl)boronic acid, after purification (ethyl acetate/methanol 9:1 v/v and ethyl acetate/methanol 8:2 v/v as eluents), yielded compound **34** as a yellow solid (88 mg, 0.22 mmol, 76%); mp 203–204 °C dec. ¹H NMR (400 MHz, DMSO-*d*₆): δ 9.48 (s, 1H), 8.58 (s, 1H), 8.18 (d, *J* = 7.2 Hz, 1H), 8.05 (d, *J* = 8.4 Hz, 2H), 7.98 (d, *J* = 7.2 Hz, 1H), 7.74 (d, *J* = 8.4 Hz, 2H), 7.64 (t, *J* = 7.6 Hz, 1H), 7.20–7.11 (m, 2H), 7.00 (d, *J* = 7.2 Hz, 1H), 3.87 (s, 3H), 3.60 (s, 3H). ¹³C NMR (101 MHz; DMSO-*d*₆): δ 168.3, 153.4, 147.3, 146.5, 138.7, 136.0 (2C), 134.2 (2C), 130.9, 129.6, 129.4, 129.3, 126.6, 124.8, 122.4, 120.4, 120.2, 113.3, 60.7, 56.3. IR (neat) $\bar{\nu}$: 3165, 2933, 2837, 1700, 1520, 1452, 1258, 1029, 791, 756 cm⁻¹. MS (ESI) *m/z*: 402 [M + H]⁺. HRMS (ESI) *m/z*: (M + H)⁺ calcd for C₂₃H₂₀N₃O₄, 402.1448; found, 402.1440. Sodium salt of **34**: mp 178–179 °C dec.

3-(1-(4-(2,3-Dihydrobenzo[*b*][1,4]dioxin-5-yl)phenyl)-1H-1,2,3-triazol-4-yl)benzoic Acid, (35). Following general procedure C, the reaction of **26** and (2,3-dihydrobenzo[*b*][1,4]dioxin-5-yl)boronic acid, after purification (ethyl petroleum ether/acetate 1:9 v/v and ethyl acetate/methanol 9:1 v/v as eluents), yielded compound **35** as a pale yellow solid (88 mg, 0.22 mmol, 76%); mp 218–220 °C dec. ¹H NMR (400 MHz, DMSO-*d*₆): δ 9.48 (s, 1H), 8.56 (s, 1H), 8.17 (d, *J* = 5.9 Hz, 1H), 8.03 (d, *J* = 8.5 Hz, 2H), 7.97 (d, *J* = 7.5 Hz, 1H), 7.76 (d, *J* = 8.5 Hz, 2H), 7.62 (t, *J* = 7.5 Hz, 1H), 6.96–6.93 (m, 3H), 4.31–4.29 (m, 4H). ¹³C NMR (101 MHz; DMSO-*d*₆): δ 167.9, 147.1, 144.4, 141.2, 138.2, 135.9, 133.1, 131.0, 130.4, 129.7, 129.6, 129.4, 129.3, 126.6, 122.6, 121.5, 120.5, 120.1, 117.4, 64.7, 64.3. IR (neat) $\bar{\nu}$: 3164, 2922, 2874, 1700, 1467, 1402, 1257, 1213, 1080, 758, 692 cm⁻¹. MS (ESI) *m/z*: 400 [M + H]⁺. HRMS (ESI) *m/z*: (M + H)⁺ calcd for C₂₃H₁₈N₃O₄, 400.1292; found, 400.1283.

3-(1-(3',5'-Dimethoxy-[1,1'-biphenyl]-4-yl)-1H-1,2,3-triazol-4-yl)-benzoic Acid, (36). Following general procedure C, the reaction of **26** and (3,5-dimethoxyphenyl)boronic acid, after purification (ethyl acetate/methanol 9:1 v/v as eluent), yielded compound **36** as a white solid (100 mg, 0.25 mmol, 86%); mp 209–210 °C. ¹H NMR (400 MHz, DMSO-*d*₆): δ 9.46 (s, 1H), 8.59 (s, 1H), 8.13 (d, *J* = 7.6 Hz, 1H), 8.06 (d, *J* = 8.2 Hz, 2H), 7.99 (d, *J* = 7.6 Hz, 1H), 7.94 (d, *J* = 8.2 Hz, 2H), 7.58 (t, *J* = 7.6 Hz, 1H), 6.89 (s, 2H), 6.55 (s, 1H), 3.84 (s, 6H). ¹³C NMR (101 MHz; DMSO-*d*₆): δ 170.7, 161.5, 147.5, 141.4, 140.7, 136.5, 130.7, 129.5, 129.3 (2C), 128.8, 128.7, 126.7, 120.7, 120.3, 105.4, 100.4, 55.8 (2C). IR (KBr) $\bar{\nu}$: 3558, 3489, 3403, 3160, 2836, 1522, 1152, 1061, 825, 757 cm⁻¹. HRMS (ESI) *m/z*: (M + H)⁺ calcd for C₂₃H₂₀N₃O₄, 402.1448; found, 402.1441. MS (ESI) *m/z*: 402 [M + H]⁺. Sodium salt of **36**: mp 169–170 °C dec.

3-(1-(3',4'-Dimethoxy-[1,1'-biphenyl]-4-yl)-1H-1,2,3-triazol-4-yl)-benzoic Acid, (37). Following general procedure C, the reaction of **26** and (3,4-dimethoxyphenyl)boronic acid, after purification (ethyl acetate/methanol 9:1 v/v and ethyl acetate/methanol 8:2 v/v as eluents), yielded compound **37** as a pale yellow solid (50 mg, 0.12 mmol, 43%); mp 244–246 °C. ¹H NMR (300 MHz, DMSO-*d*₆): δ 9.47 (s, 1H), 8.55 (s, 1H), 8.17 (d, *J* = 7.1 Hz, 1H), 8.03 (d, *J* = 8.2 Hz, 2H), 7.97–7.90 (m, 3H), 7.62 (t, *J* = 7.9 Hz, 1H), 7.33–7.29 (m, 2H), 7.07 (d, *J* = 7.9 Hz, 1H), 3.99 (s, 3H), 3.88 (s, 3H). ¹³C NMR (101 MHz; DMSO-*d*₆): δ 168.0, 149.7, 149.5, 147.1, 140.8, 135.7, 133.1, 131.9, 131.0, 130.4, 129.7, 129.4, 128.1, 126.5, 120.7, 120.5, 119.5, 112.9, 110.9, 56.2, 56.1. IR (neat) $\bar{\nu}$: 3407, 2924, 2851, 1686, 1504, 1227, 1139, 1024, 810, 757 cm⁻¹. MS (ESI) *m/z*: 402 [M + H]⁺. HRMS (ESI) *m/z*: (M + H)⁺ calcd for C₂₃H₂₀N₃O₄, 402.1448; found, 402.1442.

3-(1-(4-(2,3-Dihydrobenzo[*b*][1,4]dioxin-6-yl)phenyl)-1H-1,2,3-triazol-4-yl)benzoic Acid, (38). Following general procedure C, the reaction of **26** and (2,3-dihydrobenzo[*b*][1,4]dioxin-6-yl)boronic acid, after purification (ethyl acetate/methanol 9:1 v/v as eluent), yielded compound **38** as a white solid (87 mg, 0.22 mmol, 75%); mp 255–256 °C. ¹H NMR (400 MHz, DMSO-*d*₆): δ 9.48 (s, 1H), 8.56 (s, 1H), 8.18 (d, *J* = 7.5 Hz, 1H), 8.02 (d, *J* = 8.4 Hz, 2H), 7.96 (d, *J* = 7.5 Hz, 1H), 7.86 (d, *J* = 8.4 Hz, 2H), 7.63 (t, *J* = 7.5 Hz, 1H), 7.27–7.24 (m, 2H), 6.97 (d, *J* = 8.2 Hz, 1H), 4.30–4.29 (m, 4H). ¹³C NMR (101 MHz; DMSO-*d*₆): δ 168.0, 147.1, 144.3, 144.1, 140.3, 135.8, 133.1, 132.5, 131.0, 129.7, 129.6, 129.4, 127.9, 126.6, 120.7, 120.4, 120.1, 118.1, 115.7, 64.7, 64.6. IR (KBr) $\bar{\nu}$: 3124, 2873, 1862, 1504, 1302, 1230, 1069, 812, 562 cm⁻¹. MS (ESI) *m/z*: 400 [M + H]⁺. HRMS (ESI) *m/z*: (M + H)⁺ calcd for C₂₃H₁₈N₃O₄, 400.1292; found, 400.1286. Sodium salt of **38**: mp 196–197 °C dec.

3-(1-(4-(Benzo[*d*][1,3]dioxol-5-yl)phenyl)-1H-1,2,3-triazol-4-yl)-benzoic Acid, (39). Following general procedure C, the reaction of **26** and benzo[*d*][1,3]dioxol-5-ylboronic acid, after purification (ethyl acetate/methanol 9:1 v/v as eluent), yielded compound **39** as a yellow solid (37 mg, 0.10 mmol, 33%); mp 263–264 °C. ¹H NMR (300 MHz, DMSO-*d*₆): δ 9.51 (s, 1H), 8.54 (s, 1H), 8.17 (d, *J* = 7.4 Hz, 1H), 8.03 (d, *J* = 8.5 Hz, 2H), 7.95 (d, *J* = 7.9 Hz, 1H), 7.87 (d, *J* = 8.5 Hz, 2H), 7.61 (t, *J* = 7.4 Hz, 1H), 7.42 (s, 1H), 7.27 (d, *J* = 7.9 Hz, 1H), 7.04 (d, *J* = 7.4 Hz, 1H), 6.09 (s, 2H). ¹³C NMR (101 MHz; DMSO-*d*₆): δ 168.3, 148.7, 147.8, 147.3, 140.8, 135.9, 133.6, 131.1, 130.5, 129.7, 129.5, 128.3, 126.6, 121.1, 120.1, 120.5, 109.3, 107.7, 101.9, 79.8. IR (KBr) $\bar{\nu}$: 3930, 3552, 3480, 3414, 2922, 1501, 1228, 1041, 936, 812, 614 cm⁻¹. MS (ESI) *m/z*: 386 [M + H]⁺. HRMS (ESI) *m/z*: (M + H)⁺ calcd for C₂₂H₁₆N₃O₄, 386.1135; found, 386.1129.

3-(1-(2'-Fluoro-5'-methoxy-[1,1'-biphenyl]-4-yl)-1H-1,2,3-triazol-4-yl)benzoic Acid, (40). Following general procedure C, the reaction of **26** and (2-fluoro-5-methoxyphenyl)boronic acid, after purification (ethyl acetate/methanol 9:1 v/v as eluent), yielded compound **40** as a white solid (52 mg, 0.13 mmol, 46%); mp 223–225 °C. ¹H NMR (400 MHz, DMSO-*d*₆): δ 9.45 (s, 1H), 8.54 (s, 1H), 8.16 (d, *J* = 7.1 Hz, 1H), 8.08 (d, *J* = 7.8 Hz, 2H), 7.95 (d, *J* = 7.1 Hz, 1H), 7.82 (d, *J* = 7.8 Hz, 2H), 7.64 (t, *J* = 7.8 Hz, 1H), 7.29 (t, *J* = 9.2 Hz, 1H), 7.14 (dd, *J*_s = 6.4, 3.2 Hz, 1H), 7.03–6.99 (m, 1H), 3.83 (s, 3H). ¹³C NMR (101 MHz; DMSO-*d*₆): δ 167.9, 156.3, 155.1, 152.7, 147.2, 136.5, 135.8, 132.9, 131.0, 130.8, 129.6, 129.5, 128.1 (d, *J* = 316.3 Hz), 127.9 (d, *J* = 15.1 Hz), 120.6, 120.5, 117.5 (d, *J* = 24.6 Hz), 115.6 (d, *J* = 3.0 Hz), 115.5 (d, *J* = 8.4 Hz), 56.2. IR (neat) $\bar{\nu}$: 3407, 2923, 1686, 1613, 1502, 1228, 1024, 808, 756, 611 cm⁻¹. MS (ESI) *m/z*: 390 [M + H]⁺. HRMS (ESI) *m/z*: (M + H)⁺ calcd for C₂₂H₁₇FN₃O₃, 390.1248; found, 390.1241. Sodium salt of **40**: mp 191–192 °C dec.

1-Bromo-4-ethynylbenzene, (41). To a solution of 4-bromobenzaldehyde (2.15 g, 11.62 mmol) in MeOH (22 mL) K₂CO₃ (3.21 g, 23.24 mmol) and dimethyl (1-diazo-2-oxopropyl)phosphonate (2.61 g, 17.43 mmol) were added in order under nitrogen atmosphere. The mixture was stirred at room temperature overnight, then the solvent was removed under vacuum, water was added, and the aqueous layer was extracted with CH₂Cl₂ (5×). The organic phases were collected, dried over sodium sulfate, and evaporated. Purification by column chromatography (petroleum ether/ethyl acetate 9:1 and petroleum ether/ethyl acetate 8:2 v/v as eluents) yielded compound **41** as an orange solid (1.12 g, 6.26 mmol, 54%); ¹H NMR (300 MHz, CDCl₃): δ 7.45 (d, *J* = 8.5 Hz, 2H), 7.34 (d, *J* = 8.5 Hz, 2H), 3.11 (s, 1H). MS (ESI) *m/z*: 180 [M + H]⁺.

3-(4-(4-Bromophenyl)-1H-1,2,3-triazol-1-yl)benzoic Acid, (43). To a suspension of 1-bromo-4-ethynylbenzene (1 g, 5.52 mmol) in water (6 mL) and *t*-BuOH (6 mL) 3-azidobenzoic acid (0.89 g, 5.52 mmol) was added. Then, 55 μL of an aqueous solution of sodium ascorbate 1M and copper sulfate pentahydrate (13.7 mg, 0.055 mmol) were added and the mixture was vigorously stirred overnight. Evaporation and purification by column chromatography (petroleum ether/ethyl acetate 3:7 v/v and ethyl acetate as eluents) yielded compound **43** as a pale yellow solid (1.23 g, 3.59 mmol, 65%); ¹H NMR (300 MHz, DMSO-*d*₆): δ 9.50 (s, 1H), 8.46 (s, 1H), 8.19 (d, *J*

= 7.6 Hz, 1H), 8.06 (d, $J = 7.6$ Hz, 1H), 7.92 (d, $J = 8.5$ Hz, 2H), 7.78–7.69 (m, 3H). MS (ESI) m/z : 343 [M – H][–].

General Procedure D. Compounds 44–56 were prepared from a solution of 43 (0.29 mmol, 1 equiv) in DMF (750 μ L) and ethanol (750 μ L) under nitrogen atmosphere in the presence of the relative boronic acid (0.44 mmol, 1.5 equiv). Reactions were carried out at 80 °C overnight in the presence of Pd(OAc)₂ (0.0029 mmol, 0.01 equiv) and K₂CO₃ (0.58 mmol, 2 equiv). After filtration of the reaction mixture under vacuo over a pad of celite and evaporation of the volatile, purification by silica gel column chromatography was performed.

3-(4-([1,1'-Biphenyl]-4-yl)-1H-1,2,3-triazol-1-yl)benzoic Acid, (44). Following general procedure D, the reaction of 43 and phenylboronic acid, after purification (ethyl acetate as eluent), yielded compound 44 as a white solid (54 mg, 0.16 mmol, 55%); mp 205–206 °C. ¹H NMR (300 MHz, DMSO-*d*₆): δ 9.48 (s, 1H), 8.48 (s, 1H), 8.13–8.03 (m, 5H), 7.83–7.69 (m, 4H), 7.49 (m, 2H), 7.38 (d, $J = 7.1$ Hz, 1H). ¹³C NMR (101 MHz; DMSO-*d*₆): δ 168.2, 147.6, 140.3, 140.0, 136.9, 130.2, 129.8, 129.7, 129.5, 128.1, 127.7, 127.0, 126.4, 125.9, 122.9, 120.9, 120.3. IR (KBr) $\bar{\nu}$: 3104, 2852, 1480, 1399, 1324, 1231, 912, 761, 724 cm^{–1}. MS (ESI) m/z : 342 [M + H]⁺. HRMS (ESI) m/z : (M + H)⁺ calcd for C₂₁H₁₆N₃O₂, 342.1237; found, 342.1230.

3-(4-(2'-Methoxy-1,1'-biphenyl)-4-yl)-1H-1,2,3-triazol-1-yl)benzoic Acid, (45). Following general procedure D, the reaction of 43 and phenylboronic acid, after purification (ethyl acetate as eluent), yielded compound 45 as a white solid (24 mg, 0.06 mmol, 22%). The title compound was synthesized following general procedure D starting from compound 43 and (2-methoxyphenyl)boronic acid. The crude material was purified by column chromatography using ethyl acetate/methanol 9:1 v/v as eluent, yielding compound 45 as a white solid (24 mg, 0.06 mmol, 22%); mp 222–223 °C. ¹H NMR (300 MHz, DMSO-*d*₆): δ 9.41 (s, 1H), 8.51 (s, 1H), 8.19 (d, $J = 7.7$ Hz, 1H), 8.00 (d, $J = 7.7$ Hz, 1H), 7.71–7.62 (m, 3H), 7.37–7.35 (m, 3H), 7.13–7.05 (m, 3H), 3.81 (s, 3H). ¹³C NMR (101 MHz, DMSO-*d*₆): δ 168.1, 156.7, 147.8, 138.5, 137.1, 130.7, 130.4, 130.3, 129.7, 129.7, 129.5, 129.2, 125.5, 123.4, 121.3, 120.9, 120.2, 112.3, 56.0. IR (KBr) $\bar{\nu}$: 3126, 2932, 1658, 1599, 1456, 1323, 1251, 763, 709 cm^{–1}. MS (ESI) m/z : 372 [M + H]⁺. HRMS (ESI) m/z : (M + H)⁺ calcd for C₂₂H₁₈N₃O₃, 372.1343; found, 372.1346.

3-(4-(2',4'-Dimethoxy-1,1'-biphenyl)-4-yl)-1H-1,2,3-triazol-1-yl)benzoic Acid, (46). Following general procedure D, the reaction of 43 and (2,4-dimethoxyphenyl)boronic acid, after purification (ethyl acetate/methanol 9:1 v/v as eluent), yielded compound 46 as a yellow solid (114 mg, 0.28 mmol, 98%); mp 259–260 °C. ¹H NMR (300 MHz, DMSO-*d*₆): δ 9.41 (s, 1H), 8.47 (s, 1H), 8.13 (d, $J = 7.4$ Hz, 1H), 8.04 (d, $J = 7.4$ Hz, 1H), 7.96 (d, $J = 7.1$ Hz, 2H), 7.71 (d, $J = 6.6$ Hz, 1H), 7.55 (d, $J = 7.1$ Hz, 2H), 7.27 (t, $J = 7.4$ Hz, 1H), 6.67–6.61 (m, 2H), 3.80 (s, 3H), 3.78 (s, 3H). ¹³C NMR (75 MHz; DMSO-*d*₆): δ 167.6, 160.8, 157.8, 147.9, 138.5, 137.2, 135.9, 131.4, 130.5, 130.2, 129.7, 128.1, 125.6, 123.5, 122.5, 120.8, 120.1, 106.0, 99.6, 56.2, 55.9. IR (KBr) $\bar{\nu}$: 3551, 3415, 3124, 2837, 1525, 1312, 1052, 834, 686 cm^{–1}. MS (ESI) m/z : 402 [M + H]⁺. HRMS (ESI) m/z : (M + H)⁺ calcd for C₂₃H₂₀N₃O₄, 402.1448; found, 402.1440.

3-(4-(2',6'-Dimethoxy-1,1'-biphenyl)-4-yl)-1H-1,2,3-triazol-1-yl)benzoic Acid, (47). Following general procedure D, the reaction of 43 and (2,6-dimethoxyphenyl)boronic acid, after purification (ethyl acetate, ethyl acetate/methanol 9:1 v/v and ethyl acetate/methanol 8:2 v/v as eluents), yielded compound 47 as a pale yellow solid (53 mg, 0.13 mmol, 46%); mp 215–217 °C dec. ¹H NMR (300 MHz, DMSO-*d*₆): δ 9.40 (s, 1H), 8.55 (s, 1H), 8.15 (d, $J = 7.4$ Hz, 1H), 8.06 (d, $J = 7.4$ Hz, 1H), 7.96–7.92 (m, 3H), 7.72–7.70 (m, 4H), 7.29 (t, $J = 7.4$ Hz, 1H), 3.69 (s, 6H). ¹³C NMR (100.1 MHz, DMSO-*d*₆): δ = 167.4, 157.6, 146.9, 137.0, 132.4, 131.9, 130.6, 130.0, 129.8, 129.4, 127.8, 125.9, 125.1, 123.7, 121.8, 120.8, 105.0, 56.2. IR (neat) $\bar{\nu}$: 3409, 2920, 2850, 1686, 1399, 1227, 1009, 816, 756, 502 cm^{–1}. MS (ESI) m/z : 402 [M + H]⁺. HRMS (ESI) m/z : (M + H)⁺ calcd for C₂₃H₂₀N₃O₄, 402.1448; found, 402.1443.

3-(4-(3'-Methoxy-1,1'-biphenyl)-4-yl)-1H-1,2,3-triazol-1-yl)benzoic Acid, (48). Following general procedure D, the reaction of 43

and (3-methoxyphenyl)boronic acid, after purification (ethyl acetate/methanol 9:1 v/v as eluent), yielded compound 48 as a white solid (66 mg, 0.18 mmol, 61%); mp 216–217 °C. ¹H NMR (300 MHz, DMSO-*d*₆): δ 9.53 (s, 1H), 8.50 (s, 1H), 8.25 (d, $J = 7.7$ Hz, 1H), 8.07–8.05 (m, 3H), 7.84–7.75 (m, 3H), 7.40–7.27 (m, 3H), 6.96 (d, $J = 7.7$, 1H), 3.84 (s, 3H). ¹³C NMR (101 MHz, DMSO-*d*₆): δ 166.9, 160.3, 147.7, 141.5, 140.3, 137.3, 133.3, 130.9, 130.5, 129.9, 129.7, 127.8, 126.3, 124.4, 120.8, 120.3, 119.4, 113.8, 112.5, 55.7. IR (KBr) $\bar{\nu}$: 3134, 2923, 1689, 1592, 1462, 1319, 1225, 758, 717 cm^{–1}. MS (ESI) m/z : 372 [M + H]⁺. HRMS (ESI) m/z : (M + H)⁺ calcd for C₂₂H₁₈N₃O₃, 372.1343; found, 372.1338.

3-(4-(3'-(Methylthio)-[1,1'-biphenyl]-4-yl)-1H-1,2,3-triazol-1-yl)benzoic Acid, (49). Following general procedure D, the reaction of 43 and (3-(methylthio)phenyl)boronic acid, after purification (petroleum ether/ethyl acetate 5:5 v/v as eluent), yielded compound 49 as a yellowish solid (111 mg, 0.29 mmol, 99%); mp 225–226 °C. ¹H NMR (300 MHz, DMSO-*d*₆): δ 9.49 (s, 1H), 8.47 (s, 1H), 8.13–8.03 (m, 4H), 7.83 (d, $J = 8.3$ Hz, 2H), 7.70 (d, $J = 7.7$ Hz, 1H), 7.58 (s, 1H), 7.51 (d, $J = 7.1$ Hz, 1H), 7.43 (t, $J = 7.7$ Hz, 1H), 7.28 (d, $J = 7.7$ Hz, 1H), 2.56 (s, 3H). ¹³C NMR (101 MHz, DMSO-*d*₆): δ 168.2, 147.5, 140.8, 139.8, 139.5, 137.2, 137.0, 130.2, 130.1, 129.9, 129.7, 127.8, 126.4, 125.6, 124.3, 123.7, 123.0, 120.9, 120.3, 15.2. IR (KBr) $\bar{\nu}$: 3525, 3127, 2825, 1688, 1593, 1304, 1043, 818, 757, 696 cm^{–1}. MS (ESI) m/z : 386 [M-H][–]. HRMS (ESI) m/z : (M + H)⁺ calcd for C₂₂H₁₈N₃O₂S, 388.1114; found, 388.1107.

3-(4-(2',3'-Dimethoxy-1,1'-biphenyl)-4-yl)-1H-1,2,3-triazol-1-yl)benzoic Acid, (50). Following general procedure D, the reaction of 43 and (2,3-dimethoxyphenyl)boronic acid, after purification (ethyl acetate/methanol 9:1 v/v and ethyl acetate/methanol 8:2 v/v as eluents), yielded compound 50 as a white solid (88 mg, 0.22 mmol, 76%); mp 189–190 °C dec. ¹H NMR (400 MHz, DMSO-*d*₆): δ 9.45 (s, 1H), 8.53 (s, 1H), 8.12–8.04 (m, 4H), 7.70–7.60 (m, 3H), 7.14–6.97 (m, 3H), 3.85 (s, 3H), 3.57 (s, 3H). ¹³C NMR (101 MHz, DMSO-*d*₆): δ 168.3, 153.4, 147.7, 146.5, 138.2, 137.0, 136.8, 135.0, 130.3, 130.0, 129.7, 129.5, 125.7, 124.7, 123.1, 122.4, 120.9, 120.3, 113.0, 60.6, 56.3. IR (neat) $\bar{\nu}$: 3410, 2929, 2834, 1687, 1539, 1400, 1259, 1003, 757, 709, 583 cm^{–1}. MS (ESI) m/z : 402 [M + H]⁺. HRMS (ESI) m/z : (M + H)⁺ calcd for C₂₃H₂₀N₃O₄, 402.1448; found, 402.1440.

3-(4-(4-(2,3-Dihydrobenzo[b][1,4]dioxin-5-yl)phenyl)-1H-1,2,3-triazol-1-yl)benzoic Acid, (51). Following general procedure D, the reaction of 43 and (2,3-dihydrobenzo[b][1,4]dioxin-5-yl)boronic acid, after purification (ethyl acetate/methanol 9:1 v/v and ethyl acetate/methanol 8:2 v/v as eluents), yielded compound 51 as a pale yellow solid (105 mg, 0.26 mmol, 91%); mp 186–188 °C dec. ¹H NMR (300 MHz, DMSO-*d*₆): δ 9.42 (s, 1H), 8.49 (s, 1H), 8.11–7.99 (m, 4H), 7.70 (t, $J = 7.2$ Hz, 1H), 7.63 (d, $J = 7.4$ Hz, 2H), 6.93–6.90 (m, 3H), 4.29–4.26 (m, 4H). ¹³C NMR (101 MHz, DMSO-*d*₆): δ 167.6, 147.8, 144.3, 141.1, 137.7, 137.1, 132.4, 130.5, 130.2, 130.1, 129.4, 127.8, 125.5, 123.7, 122.6, 121.4, 120.8, 120.3, 117.1, 64.6, 64.3. IR (neat) $\bar{\nu}$: 3408, 2921, 2873, 1687, 1466, 1400, 1238, 1042, 872, 778 cm^{–1}. MS (ESI) m/z : 400 [M + H]⁺. HRMS (ESI) m/z : (M + H)⁺ calcd for C₂₃H₁₈N₃O₄, 400.1292; found, 400.1287.

3-(4-(3',5'-Dimethoxy-1,1'-biphenyl)-4-yl)-1H-1,2,3-triazol-1-yl)benzoic Acid, (52). Following general procedure D, the reaction of 43 and (3,5-dimethoxyphenyl)boronic acid, after purification (ethyl acetate/methanol 9:1 v/v as eluent), yielded compound 52 as a yellow solid (115 mg, 0.29 mmol, 99%); mp 253–254 °C. ¹H NMR (300 MHz, DMSO-*d*₆): δ 9.50 (s, 1H), 8.50 (s, 1H), 8.14 (d, $J = 7.1$ Hz, 1H), 8.06–8.04 (m, 3H), 7.82 (d, $J = 8.2$ Hz, 2H), 7.70 (t, $J = 7.1$ Hz, 1H), 6.94–6.87 (m, 2H), 6.52 (s, 1H), 3.82 (s, 3H), 3.78 (s, 3H). ¹³C NMR (101 MHz; DMSO-*d*₆): δ 167.9, 161.4, 160.3, 147.6, 142.2, 140.2, 137.1, 130.4, 130.0, 129.7, 127.8, 126.3, 123.3, 120.8, 120.3 (2C), 111.9, 105.2, 100.1, 55.8, 55.4. IR (KBr) $\bar{\nu}$: 3140, 2838, 1503, 1353, 1204, 1154, 820, 690 cm^{–1}. MS (ESI) m/z : 402 [M + H]⁺. HRMS (ESI) m/z : (M + H)⁺ calcd for C₂₃H₂₀N₃O₄, 402.1448; found, 402.1439.

3-(4-(3',4'-Dimethoxy-1,1'-biphenyl)-4-yl)-1H-1,2,3-triazol-1-yl)benzoic Acid, (53). Following general procedure D, the reaction of 43 and (3,4-dimethoxyphenyl)boronic acid, after purification (ethyl

acetate/methanol 9:1 v/v and ethyl acetate/methanol 8:2 v/v as eluents), yielded compound **53** as a white solid (65 mg, 0.16 mmol, 56%); mp 253–254 °C dec. ¹H NMR (300 MHz, DMSO-*d*₆): δ 9.41 (s, 1H), 8.49 (s, 1H), 8.16 (d, *J* = 7.9 Hz, 1H), 8.08–8.02 (m, 3H), 7.79 (d, *J* = 8.0 Hz, 2H), 7.71 (t, *J* = 7.9 Hz, 1H), 7.30–7.27 (m, 2H), 7.06 (d, *J* = 7.9 Hz, 1H), 3.88 (s, 3H), 3.82 (s, 3H). ¹³C NMR (101 MHz, DMSO): δ 168.2, 149.6, 149.2, 147.7, 140.3, 137.0, 132.8, 132.4, 130.3, 129.1, 127.8, 127.3, 126.3, 123.2, 120.9, 120.1, 119.3, 112.7, 110.8, 56.2, 56.1. IR (neat) $\bar{\nu}$: 3408, 2927, 1686, 1519, 1399, 1248, 1139, 1011, 804, 757 cm⁻¹. MS (ESI) *m/z*: 402 [M + H]⁺. HRMS (ESI) *m/z*: (M + H)⁺ calcd for C₂₃H₂₀N₃O₄, 402.1448; found, 402.1444.

3-(4-(4-(2,3-Dihydrobenzo[*b*][1,4]dioxin-6-yl)phenyl)-1H-1,2,3-triazol-1-yl)benzoic Acid, (54). Following general procedure D, the reaction of **43** and (2,3-dihydrobenzo[*b*][1,4]dioxin-6-yl)boronic acid, after purification (ethyl acetate as eluent), yielded compound **54** as a pale yellow solid (115 mg, 0.29 mmol, 99%); mp 192–193 °C. ¹H NMR (300 MHz, DMSO-*d*₆): δ 9.49 (s, 1H), 8.49 (s, 1H), 8.22 (d, *J* = 8.0 Hz, 1H), 8.02 (d, *J* = 8.5 Hz, 2H), 7.79–7.77 (m, 3H), 7.27–7.22 (m, 3H), 6.95 (d, *J* = 8.0 Hz, 1H), 4.34–4.28 (m, 4H). ¹³C NMR (101 MHz; DMSO-*d*₆): δ 167.1, 147.7, 145.6, 144.2, 143.8, 143.2, 139.8, 137.2, 133.3, 130.7, 128.0, 127.2, 126.3, 123.3, 120.1, 119.9, 117.9, 116.6, 115.5, 64.7, 64.6. IR (KBr) $\bar{\nu}$: 2880, 2362, 1676, 1483, 1420, 1311, 1252, 800, 752 cm⁻¹. MS (ESI) *m/z*: 400 [M + H]⁺. HRMS (ESI) *m/z*: (M + H)⁺ calcd for C₂₃H₁₈N₃O₄, 400.1292; found, 400.1286.

3-(4-(4-(Benzo[*d*][1,3]dioxol-5-yl)phenyl)-1H-1,2,3-triazol-1-yl)benzoic Acid, (55). Following general procedure D, the reaction of **43** and benzo[*d*][1,3]dioxol-5-ylboronic acid, after purification (ether/ethyl acetate 1:9 v/v as eluent), yielded compound **55** as a yellowish solid (65 mg, 0.17 mmol, 58%); mp 270–271 °C. ¹H NMR (300 MHz, DMSO-*d*₆): δ 9.48 (s, 1H), 8.49 (s, 1H), 8.22 (d, *J* = 8.2 Hz, 1H), 8.05–7.94 (m, 3H), 7.79–7.74 (m, 3H), 7.33 (s, 1H), 7.23 (t, *J* = 8.2 Hz, 1H), 7.02 (d, *J* = 8.2 Hz, 1H), 6.11 (s, 2H). ¹³C NMR (101 MHz; DMSO-*d*₆): δ 166.9, 148.5, 147.7, 147.5, 140.1, 137.3, 134.3, 132.5, 130.8, 129.7, 127.8, 127.4, 126.3, 124.3, 120.7, 120.2, 109.1, 107.4, 101.7, 79.8. IR (KBr) $\bar{\nu}$: 3109, 2900, 1736, 1480, 1399, 1322, 1233, 932, 803 cm⁻¹. MS (ESI) *m/z*: 386 [M + H]⁺. HRMS (ESI) *m/z*: (M + H)⁺ calcd for C₂₂H₁₆N₃O₄, 386.1135; found, 386.1129.

3-(4-(2'-Fluoro-5'-methoxy-[1,1'-biphenyl]-4-yl)-1H-1,2,3-triazol-1-yl)benzoic Acid, (56). Following general procedure D, the reaction of **43** and (2-fluoro-5-methoxyphenyl)boronic acid, after purification (petroleum ether/ethyl acetate 2:8 v/v as eluent), yielded compound **56** as a yellow solid (46 mg, 0.12 mmol, 41%); mp 149–150 °C dec. ¹H NMR (400 MHz, DMSO-*d*₆): δ 9.52 (s, 1H), 8.51 (s, 1H), 8.25 (d, *J* = 8.0 Hz, 1H), 8.09–8.07 (m, 3H), 7.79 (t, *J* = 7.9 Hz, 1H), 7.72 (d, *J* = 8.0 Hz, 2H), 7.27 (t, *J* = 9.2 Hz, 1H), 7.14 (dd, *J*_s = 6.4, 3.2 Hz, 1H), 7.00–6.96 (m, 1H), 3.83 (s, 3H). ¹³C NMR (101 MHz; DMSO-*d*₆): δ 166.9, 156.2, 155.1, 152.7, 147.6, 137.2, 133.9 (d, *J* = 300.0 Hz), 130.9, 129.9, 129.8, 128.7 (d, *J* = 14.6 Hz), 127.8, 126.0, 124.4, 120.6, 120.5, 117.4 (d, *J* = 24.8 Hz), 115.5 (d, *J* = 3.0 Hz), 115.2 (d, *J* = 8.5 Hz), 56.2. IR (neat) $\bar{\nu}$: 2921, 2581, 2668, 1675, 1480, 1298, 1206, 1038, 807, 752, 674 cm⁻¹. MS (ESI) *m/z*: 390 [M + H]⁺. HRMS (ESI) *m/z*: (M + H)⁺ calcd for C₂₂H₁₇FN₃O₃, 390.1249; found, 390.1240.

4-(2,3-Dihydrobenzo[*b*][1,4]dioxin-6-yl)aniline, (61). To a solution of 4-bromoaniline **6** (300 mg, 1.74 mmol) in ethanol (1.5 mL) and DMF (1.5 mL), (2,3-dihydrobenzo[*b*][1,4]dioxin-6-yl)boronic acid **60** (313 mg, 1.74 mmol), Pd(OAc)₂ (11.7 mg, 0.017 mmol) and K₂CO₃ (481 mg, 3.48 mmol) were added in order. The mixture was heated at 80 °C for 6 h and then was left at rt overnight. The mixture was filtered over a pad of celite and rinsed with methanol and then the volatile was removed. Purification by column chromatography (petroleum ether/ethyl acetate 8:2 v/v as eluent) yielded compound **61** as a dark yellow oil (339 mg, 1.49 mmol, 86%); ¹H NMR (300 MHz, CDCl₃): δ = 7.38 (d, *J* = 8.2 Hz, 2H), 7.11 (s, 1H), 7.06 (d, *J* = 8.5 Hz, 1H), 6.94 (d, *J* = 8.5 Hz, 1H), 6.72 (d, *J* = 8.2 Hz, 2H), 4.28–4.27 (m, 4H). MS (ESI) *m/z*: 228 [M + H]⁺.

Methyl 3-((4-(2,3-Dihydrobenzo[*b*][1,4]dioxin-6-yl)phenyl)-carbamoyl)benzoate, (63). To a solution of compound **61** (320

mg, 1.41 mmol) in dry CH₂Cl₂ (6.4 mL), 3-(methoxycarbonyl)benzoic acid **62** (254 mg, 1.41 mmol), 1-ethyl-3-(3-dimethylaminopropyl)carbodiimide (EDCI) (540 mg, 2.82 mmol), DIPEA (723 μL, 4.22 mmol), and 4-dimethylaminopyridine (DMAP) (17 mg, 0.14 mmol) were added in order under nitrogen atmosphere. The reaction was stirred at rt overnight. Then, the mixture was diluted with CH₂Cl₂ and washed with HCl 3 N (3×). The organic layer was dried over sodium sulfate and evaporated. Purification by column chromatography (petroleum ether/ethyl acetate 8:2 v/v as eluent) yielded compound **63** as a pale yellow solid (424 mg, 1.09 mmol, 77%); ¹H NMR (300 MHz, CDCl₃): δ = 8.49 (br s, 1H), 8.21 (d, *J* = 6.3 Hz, 1H), 8.14 (d, *J* = 6.3 Hz, 1H), 7.98 (s, 1H), 7.70 (d, *J* = 7.1 Hz, 2H), 7.62–7.50 (m, 3H), 7.09 (d, *J* = 7.1 Hz, 2H), 6.93 (d, *J* = 7.4 Hz, 1H), 4.29–4.28 (m, 4H), 3.96 (s, 3H). MS (ESI) *m/z*: 390 [M + H]⁺.

3-((4-(2,3-Dihydrobenzo[*b*][1,4]dioxin-6-yl)phenyl)carbamoyl)benzoic Acid, (64). Compound **63** (250 mg, 0.64 mmol) was solubilized in THF (2.8 mL). Then, a solution of NaOH (26 mg, 0.64 mmol) in water (2.8 mL) was added and the mixture was heated at 60 °C for 3 h. Water was then added and the aqueous phase extracted with ethyl acetate (3×). The organic layers were dried over sodium sulfate and evaporated. Purification by column chromatography (ethyl acetate/methanol 8:2 v/v as eluent) yielded compound **64** as a white solid (195 mg, 0.52 mmol, 81%); mp 227–228 °C dec. ¹H NMR (300 MHz, DMSO-*d*₆): δ 10.44 (br s, 1H), 8.53 (s, 1H), 8.14–8.12 (m, 2H), 7.84 (d, *J* = 8.0 Hz, 2H), 7.64–7.58 (m, 3H), 7.15–7.13 (m, 2H), 6.92 (d, *J* = 8.2 Hz, 1H), 4.28–4.27 (m, 4H). ¹³C NMR (101 MHz, DMSO-*d*₆): δ 168.8, 165.5, 144.1, 143.3, 138.6, 135.5, 135.4, 133.6, 132.7, 131.6, 129.0, 128.9, 126.8, 121.2, 119.6, 117.9, 115.2 (2C), 64.6 (2C). IR (neat) $\bar{\nu}$: 3282, 2922, 1686, 1647, 1495, 1299, 1245, 1072, 801, 695, 527 cm⁻¹. MS (ESI) *m/z*: 376 [M + H]⁺. HRMS (ESI) *m/z*: (M + H)⁺ calcd for C₂₂H₁₈NO₅, 376.1179; found, 376.1173.

4-(2,3-Dihydrobenzo[*b*][1,4]dioxin-6-yl)benzoic Acid, (66). Methyl 4-iodobenzoate **65** (200 mg, 0.76 mmol) was solubilized in ethanol (1.7 mL) and DMF (1.7 mL) under nitrogen atmosphere. (2,3-Dihydrobenzo[*b*][1,4]dioxin-6-yl)boronic acid **60** (137 mg, 0.76 mmol), Pd(OAc)₂ (5.1 mg, 0.0076 mmol), and K₂CO₃ (211 mg, 1.53 mmol) were added in order. The mixture was heated at 80 °C for 6 h and then was left at rt overnight. The reaction was filtered over a pad of celite and rinsed with methanol and then the volatile was removed, yielding a dark yellow solid. The crude product was used in the next step without further purification. The intermediate was solubilized in THF (2.4 mL) and a solution of NaOH (31 mg, 0.76 mmol) in water (2.4 mL) was added. The mixture was heated at 60 °C for 4 h, then HCl 3 N was added until pH 4, and the aqueous layer was extracted with ethyl acetate (×2). The organic layers were dried over sodium sulfate and evaporated, yielding compound **66** as a white solid (166 mg, 0.65 mmol, 85%); ¹H NMR (300 MHz, CD₃OD): δ = 8.02 (d, *J* = 7.1 Hz, 2H), 7.56 (d, *J* = 7.1 Hz, 2H), 7.10–7.07 (m, 2H), 6.89 (d, *J* = 8.2 Hz, 1H), 4.30–4.31 (m, 4H). MS (ESI) *m/z*: 255 [M - H]⁻.

Methyl 3-(4-(2,3-Dihydrobenzo[*b*][1,4]dioxin-6-yl)benzamido)benzoate, (68). Compound **66** (165 mg, 0.64 mmol) was solubilized in dry CH₂Cl₂ (4 mL) and methyl 3-aminobenzoate **67** (97.3 mg, 0.64 mmol), EDCI (247 mg, 1.29 mmol), DIPEA (331 μL, 1.93 mmol), and DMAP (7.9 mg, 0.064 mmol) were added in order under nitrogen atmosphere. The mixture was stirred at rt overnight, then was diluted with CH₂Cl₂ and washed with HCl 3 N (×5). The organic layer was dried over sodium sulfate and evaporated. Purification by column chromatography (petroleum ether/ethyl acetate 8:2 v/v as eluent) yielded compound **68** as a pale yellow solid (157 mg, 0.40 mmol, 63%); ¹H NMR (300 MHz, CDCl₃): δ = 8.16 (s, 1H), 8.07–8.01 (m, 2H), 7.91 (d, *J* = 6.9 Hz, 2H), 7.82 (d, *J* = 6.6 Hz, 1H), 7.63 (d, *J* = 6.9 Hz, 2H), 7.45 (t, *J* = 6.6 Hz, 1H), 7.13 (d, *J* = 7.7 Hz, 1H), 6.95 (d, *J* = 7.7 Hz, 1H), 4.30–4.29 (m, 4H), 3.91 (s, 3H). MS (ESI) *m/z*: 390 [M + H]⁺.

3-(4-(2,3-Dihydrobenzo[*b*][1,4]dioxin-6-yl)benzamido)benzoic Acid, (69). Compound **68** (157 mg, 0.40 mmol) was solubilized in THF (1.7 mL) and a solution of NaOH (16.1 mg, 0.40 mmol) in water (1.7 mL) was added. The mixture was heated at 60 °C for 4 h

and then was left at rt overnight. HCl 3 N was added until pH 4 and the aqueous layer was extracted with ethyl acetate (×2). The collected organic phases were dried over sodium sulfate and evaporated. Purification by column chromatography (ethyl acetate as eluent) yielded compound **69** as a white solid (91.5 mg, 0.24 mmol, 61%); mp 234–235 °C dec. ¹H NMR (300 MHz, DMSO-*d*₆): δ 10.39 (br s, 1H), 8.44 (s, 1H), 8.06–8.00 (m, 3H), 7.77 (d, *J* = 8.2 Hz, 2H), 7.69 (d, *J* = 7.4 Hz, 1H), 7.48 (t, *J* = 7.4 Hz, 1H), 7.25 (d, *J* = 8.2 Hz, 2H), 6.98 (d, *J* = 8.2 Hz, 1H), 4.30–4.29 (m, 4H). ¹³C NMR (101 MHz, DMSO-*d*₆): δ 167.8, 165.8, 144.3, 144.2, 143.1, 139.9, 133.3, 132.7, 131.9, 129.3, 128.8, 126.5, 124.9, 124.8, 121.6, 120.3, 118.1, 115.9, 64.7, 64.6. IR (neat) $\bar{\nu}$: 3310, 2924, 1693, 1650, 1485, 1302, 1069, 811, 752, 677 cm⁻¹. MS (ESI) *m/z*: 376 [M + H]⁺. HRMS (ESI) *m/z*: (M + H)⁺ calcd for C₂₂H₁₈NO₅, 376.1179; found, 376.1172.

In Vitro Metabolism Studies. Phase I and II (glucuronidation) incubations were performed in MLMs (pooled male mouse CD-1, protein concentration: 20 mg/mL, purchased from Corning B.V. Life Sciences—Amsterdam, The Netherlands) using the procedure previously described¹⁶ with the following modifications: 5 μM substrate concentration for the determination of the residual percentage and 50 μM for **34** metabolite characterization by HRMS; when metabolic activation was studied, 3 mM GSH trapping agent was added in the incubation mixture.

Aqueous Solubility. Thermodynamic aqueous solubility was determined as follows: about 3 mg of the tested compound was weighed and dissolved in 3 mL of deionized water. After vigorous mixing by vortex followed by sonication for 5 min, the resulting supersaturated solution was shaken horizontally overnight at 25 °C. After filtration over a syringe filter (pore 0.22 μm, regenerate cellulose membrane), 100 μL of DMSO was added to 1 mL of the filtered solution. The resulting solution was further diluted in water (typically 1:10) before LC–UV analysis. Aqueous solubility was calculated comparing the filtrate peak area to those of the tested compound DMSO solutions. Solubility in aqueous media was also checked in the following vehicles at the target concentration of 6 mg/mL: saline + 10% DMSO, saline + 10% DMSO + 20% PEG400, saline + 5% ethanol.

Biology. Compounds. A 50 mM stock solution of **Synta66**, **CM4620**, **teriflunomide**, **brequinar**, and all the biphenyl triazoles synthesized was dissolved in 100% DMSO and stored at +4/–20 °C. For each experiment, working concentrations of these compounds were freshly prepared by diluting DMSO to 0.1% in different physiologic solutions according to the experimental procedures (*i.e.*, Krebs–Ringer buffer, culture medium, Locke solution).

Cell Culture and Calcium Imaging Experiments. Screening, dose–response experiments, and calcium imaging experiments were performed in HEK cells (ATCC, Rock, ville, MD, USA), as already reported elsewhere.¹⁶

3-(4,5-Dimethylthiazol-2-yl)-2,5-diphenyltetrazolium Bromide Assay. Viability assays were performed in HEK cells that were plated in 24-well plates at the density of 20,000 cells per well. After 24 h, the cells were treated for other 24 h with the selected compounds. At the end of the treatments, the medium was removed and substituted with 300 μL of MTT reagent (Sigma-Aldrich Inc., Italy) at the final concentration of 0.25 mg/mL for 60 min at 37 °C. Reactions were then stopped and the crystals were solubilized by adding isopropyl alcohol/HCl (1 M) (Sigma-Aldrich Inc., Italy), before reading the absorbance at 570 nm, using the multiplate reader Victor3 V (PerkinElmer, Milan, Italy). To evaluate the effects on the DHODH enzyme, HEK cells were treated with the selected compounds in the absence or presence of 100 μM uridine for 72 h.

PK Analysis and Analysis of Pancreatitis. All animal experiments observe the regulations in Italy (D.M. 116192) as well as the EU regulations (O.J. of E.C. L 358/1 12/18/1986). Compound **34** was injected *i.v.* at a dose of 7 mg/kg in C57BL/6 mice. Blood was collected after 5, 15, 30, 60, 120, 240, 360 min and 24 h. Aliquots of plasma samples were analyzed as previously reported.¹⁶ AP was induced in mice by *i.p.* injections of cerulein, as already reported elsewhere.¹⁶

Statistical Analysis. In *in vitro* experiments, data are presented as mean ± SEM or Median and interquartile range (IQR). The normality of data distributions was assessed using the Shapiro–Wilk test. Parametric (unpaired *t*-test and one-way analysis of variance (ANOVA) followed by Tukey's post-hoc) or nonparametric (Mann–Whitney *U* test and one-way Kruskal–Wallis *H* test followed by Dunn's post-hoc) statistical analysis was used for comparisons of data. All statistical assessments were two-sided and a value of *P* < 0.05 was considered statistically significant. Statistical analyses were performed using GraphPad Prism software (GraphPad Software, Inc., USA).

In *in vivo* experiments, results were analyzed by one-way ANOVA followed by a Bonferroni post hoc test for multiple comparisons.

■ ASSOCIATED CONTENT

Supporting Information

The Supporting Information is available free of charge at <https://pubs.acs.org/doi/10.1021/acs.jmedchem.0c01305>.

Synthesis and characterization of compounds **73**, **75**, **77**, **78**; NMR spectra of **31**, **34**, **35**, **36**, **38**, **40**, **50**, **56**; biology (effect of **Synta66**, **31**, **34**, **36**, **38**, **40**, **50**, **56** on the AUC, peak amplitude, and slope of the Ca²⁺-rise in HEK cells); *in vitro* metabolism and *in vivo* PK analysis and thermodynamic aqueous solubility (PDF)

Molecular formula strings for compounds (CSV)

■ AUTHOR INFORMATION

Corresponding Author

Tracey Pirali – Department of Pharmaceutical Sciences, Università del Piemonte Orientale, Novara 28100, Italy; ChemiCare S.r.l., Novara 28100, Italy; orcid.org/0000-0003-3936-4787; Phone: +39 0321 375852; Email: tracey.pirali@uniupo.it

Authors

Marta Serafini – Department of Pharmaceutical Sciences, Università del Piemonte Orientale, Novara 28100, Italy
Celia Cordero-Sanchez – Department of Pharmaceutical Sciences, Università del Piemonte Orientale, Novara 28100, Italy
Rosanna Di Paola – Department of Chemical, Biological, Pharmaceutical and Environmental Sciences, Università di Messina, Messina 98166, Italy
Irene P. Bhela – Department of Pharmaceutical Sciences, Università del Piemonte Orientale, Novara 28100, Italy
Silvio Aprile – Department of Pharmaceutical Sciences, Università del Piemonte Orientale, Novara 28100, Italy; orcid.org/0000-0003-4804-9543
Beatrice Purgè – Department of Pharmaceutical Sciences, Università del Piemonte Orientale, Novara 28100, Italy
Roberta Fusco – Department of Chemical, Biological, Pharmaceutical and Environmental Sciences, Università di Messina, Messina 98166, Italy
Salvatore Cuzzocrea – Department of Chemical, Biological, Pharmaceutical and Environmental Sciences, Università di Messina, Messina 98166, Italy
Armando A. Genazzani – Department of Pharmaceutical Sciences, Università del Piemonte Orientale, Novara 28100, Italy; orcid.org/0000-0003-1923-7430
Beatrice Riva – Department of Pharmaceutical Sciences, Università del Piemonte Orientale, Novara 28100, Italy; ChemiCare S.r.l., Novara 28100, Italy

Complete contact information is available at:

<https://pubs.acs.org/doi/10.1021/acs.jmedchem.0c01305>

Author Contributions

M.S. and C.C.-S. contributed equally. B.R. and T.P. contributed equally. The manuscript was written through contributions of all authors. All authors have given approval to the final version of the manuscript.

Notes

The authors declare no competing financial interest.

ACKNOWLEDGMENTS

M.S. is supported by Fondazione AIRC (Associazione Italiana per la Ricerca sul Cancro) fellowship for Italy (Rif. 22568). This work was partly funded by the Telethon Foundation (GGP19110) to A. A. G.

ABBREVIATIONS

ALL, acute lymphoblastic leukemia; AP, acute pancreatitis; AUC, area under the curve; $CDCl_3$, deuterated chloroform; CD_3OD , deuterated methanol; CH_2Cl_2 , dichloromethane; CRAC, calcium release-activated channels; DHODH, dihydroorotate dehydrogenase; DIPEA, diisopropylethylamine; DMAP, 4-dimethylaminopyridine; DMEM, Dubelcco's modified Eagle's medium; DMF, dimethylformamide; DMSO, dimethyl sulfoxide; DMSO- d_6 , deuterated dimethyl sulfoxide; EDCI, 1-ethyl-3-(3-dimethylaminopropyl) carbodiimide; EGTA, ethylene glycol-bis(β -aminoethyl ether)- N,N,N',N' -tetraacetic acid; ER, endoplasmic reticulum; EtOH, ethanol; FBS, fetal bovine serum; Fura-2, fluorescent calcium indicator 2; GSH, glutathione; H&E, hematoxylin and eosin; HEK cells, human embryonic kidney cells; HPLC, high-performance liquid chromatography; HRMS, high-resolution mass spectrometry; IC_{50} , half-maximum inhibitory concentration; IP_3R , inositol trisphosphate receptor; IR, infrared; KRB, Krebs–Ringer buffer; LC–UV, liquid chromatography–ultraviolet; MLMs, mouse liver microsomes; MeOH, methanol; mp, melting point; MTT, 3-(4,5-dimethylthiazol-2-yl)-2,5-diphenyltetrazolium bromide; NADPH, nicotinamide adenine dinucleotide phosphate; NMR, nuclear magnetic resonance; Orai, calcium release-activated calcium channel protein; PACs, pancreatic acinar cells; PEG, polyethylene glycol; PK, pharmacokinetic; SAR, structure–activity relationship; SEM, standard error of the mean; SERCA, sarco-endoplasmic reticulum calcium ATPase; SOCE, store-operated calcium entry; STIM, stromal interaction molecule; t -BHQ, *tert*-butylhydroquinone; t -BuOH, *tert*-butanol; THF, tetrahydrofuran; TLC, thin-layer chromatography; TRP, transient receptor potential channels; TRPC, transient receptor potential-canonical channels; UDPGA, uridine diphosphate glucuronic acid

REFERENCES

- (1) Lee, P. J.; Papachristou, G. I. New insights into acute pancreatitis. *Nat. Rev. Gastroenterol. Hepatol.* **2019**, *16*, 479–496.
- (2) Forsmark, C. E.; Vege, S. S.; Wilcox, C. M. Acute pancreatitis. *N. Engl. J. Med.* **2016**, *375*, 1972–1981.
- (3) (a) Gerasimenko, J. V.; Gerasimenko, O. V.; Petersen, O. H. The role of Ca^{2+} in the pathophysiology of pancreatitis. *J. Physiol.* **2014**, *592*, 269–280. (b) Gerasimenko, J. V.; Peng, S.; Tsugorka, T.; Gerasimenko, O. V. Ca^{2+} signalling underlying pancreatitis. *Cell Calcium* **2018**, *70*, 95–101.
- (4) For review articles on SOCE, see: (a) Lewis, R. S. The molecular choreography of a store-operated calcium channel. *Nature* **2007**, *446*, 284–287. (b) Putney, J. W. Store-operated calcium entry: an historical overview. *Adv. Exp. Med. Biol.* **2017**, *981*, 205–214.

(c) Stathopoulos, P. B.; Ikura, M. Store operated calcium entry: from concept to structural mechanisms. *Cell Calcium* **2017**, *63*, 3–7.

(5) (a) Putney, J. W. A model for receptor-regulated calcium entry. *Cell Calcium* **1986**, *7*, 1–12. (b) Parekh, A. B.; Putney, J. W. Store-operated calcium channels. *Physiol. Rev.* **2005**, *85*, 757–810. (c) Prakriya, M.; Lewis, R. S. Store-operated calcium channels. *Physiol. Rev.* **2015**, *95*, 1383–1436.

(6) Hoth, M.; Penner, R. Depletion of intracellular calcium stores activates a calcium current in mast cells. *Nature* **1992**, *355*, 353–356.

(7) (a) Putney, J. W. Origins of the concept of store-operated calcium entry. *Front. Biosci., Scholar Ed.* **2011**, *3*, 980–984. (b) Putney, J. W. The physiological function of store-operated calcium entry. *Neurochem. Res.* **2011**, *36*, 1157–1165. (c) Berna-Erro, A.; Woodard, G. E.; Rosado, J. A. Orais and STIMs: physiological mechanisms and disease. *J. Cell Mol. Med.* **2012**, *16*, 407–424.

(8) (a) Ong, H. L.; Ambudkar, I. S. Molecular determinants of TRPC1 regulation within ER-PM junctions. *Cell Calcium* **2015**, *58*, 376–386. (b) Ong, H. L.; de Souza, L. B.; Ambudkar, I. S. Role of TRPC channels in store-operated calcium entry. *Adv. Exp. Med. Biol.* **2016**, *898*, 87–109.

(9) Kim, M. S.; Lee, K. P.; Yang, D.; Shin, D. M.; Abramowitz, J.; Kiyonaka, S.; Birnbaumer, L.; Mori, Y.; Muallem, S. Genetic and pharmacologic inhibition of the Ca^{2+} influx channel TRPC3 protects secretory epithelia from Ca^{2+} -dependent toxicity. *Gastroenterology* **2011**, *140*, 2107–2115.

(10) (a) Lur, G.; Sherwood, M. W.; Ebisui, E.; Haynes, L.; Feske, S.; Sutton, R.; Burgoyne, R. D.; Mikoshiba, K.; Petersen, O. H.; Tepikin, A. V. IP_3 receptors and Orai channels in pancreatic acinar cells: colocalization and its consequences. *Biochem. J.* **2011**, *436*, 231–239. (b) Gukovskaya, A. S.; Pandol, S. J.; Gukovsky, I. New insights into the pathways initiating and driving pancreatitis. *Curr. Opin. Gastroenterol.* **2016**, *32*, 429–435.

(11) Gerasimenko, J. V.; Gryshchenko, O.; Ferdek, P. E.; Stapleton, E.; Hebert, T. O. G.; Bychkova, S.; Peng, S.; Begg, M.; Gerasimenko, O. V.; Petersen, O. H. Ca^{2+} release-activated Ca^{2+} channel blockade as a potential tool in antipancreatitis therapy. *Proc. Natl. Acad. Sci. U.S.A.* **2013**, *110*, 13186–13191.

(12) (a) Wen, L.; Voronina, S.; Javed, M. A.; Awais, M.; Szatmary, P.; Latawiec, D.; Chvanov, M.; Collier, D.; Huang, W.; Barrett, J.; Begg, M.; Stauderman, K.; Roos, J.; Grigoryev, S.; Ramos, S.; Rogers, E.; Whitten, J.; Velicelebi, G.; Dunn, M.; Tepikin, A. V.; Criddle, D. N.; Sutton, R. Inhibitors of ORAI1 prevent cytosolic calcium-associated injury of human pancreatic acinar cells and acute pancreatitis in 3 mouse models. *Gastroenterology* **2015**, *149*, 481–492. (b) Waldron, R. T.; Chen, Y.; Pham, H.; Go, A.; Su, H. Y.; Hu, C.; Wen, L.; Husain, S. Z.; Sugar, C. A.; Roos, J.; Ramos, S.; Lugea, A.; Dunn, M.; Stauderman, K.; Pandol, S. J. The Orai Ca^{2+} channel inhibitor CM4620 targets both parenchymal and immune cells to reduce inflammation in experimental acute pancreatitis. *J. Physiol.* **2019**, *597*, 3085–3105.

(13) CM4620 Injectable Emulsion Versus Supportive Care in Patients With Acute Pancreatitis and SIRS. [ClinicalTrials.gov](https://clinicaltrials.gov/Identifier/NCT03401190). Identifier: NCT03401190. Last update: May 3, 2019 (accessed Sep 13, 2020); (b) Study of CM4620 to Reduce the Severity of Pancreatitis Due to Asparaginase. [ClinicalTrials.gov](https://clinicaltrials.gov/Identifier/NCT04195347). Identifier: NCT04195347. Last update: September 10, 2020 (accessed Sep 13, 2020).

(14) Peng, S.; Gerasimenko, J. V.; Tsugorka, T.; Gryshchenko, O.; Samarasinghe, S.; Petersen, O. H.; Gerasimenko, O. V. Calcium and adenosine triphosphate control of cellular pathology: asparaginase-induced pancreatitis elicited via protease-activated receptor 2. *Philos. Trans. R. Soc. London, Ser. B* **2016**, *371*, 20150423.

(15) For review articles on SOCE modulators, see: (a) Sweeney, Z. K.; Minatti, A.; Button, D. C.; Patrick, S. Small-molecule inhibitors of store-operated calcium entry. *ChemMedChem* **2009**, *4*, 706–718. (b) Sweeney, Z. K.; Minatti, A.; Button, D. C.; Patrick, S. Small-molecule inhibitors of store-operated calcium entry. *ChemMedChem* **2009**, *4*, 706–718. (c) Tia, C.; Du, L.; Zhou, Y.; Li, M. Store-operated CRAC channel inhibitors: opportunities and challenges.

Future Med. Chem. **2016**, *8*, 817–832. (d) Lopez, J. J.; Albarran, L.; Gómez, L. J.; Smani, T.; Salido, G. M.; Rosado, J. A. Molecular modulators of store-operated calcium entry. *Biochim. Biophys. Acta* **2016**, *1863*, 2037–2043. (e) Stauderman, K. A. CRAC channels as targets for drug discovery and development. *Cell Calcium* **2018**, *74*, 147–159.

(16) (a) Riva, B.; Griglio, A.; Serafini, M.; Cordero-Sanchez, C.; Aprile, S.; Di Paola, R.; Gugliandolo, E.; Alansary, D.; Biocotino, I.; Lim, D.; Giosa, G.; Galli, U.; Niemeyer, B.; Sorba, G.; Canonico, P. L.; Cuzzocrea, S.; Genazzani, A. A.; Pirali, T. Pyrtriazoles, a novel class of store-operated calcium entry modulators: discovery, biological profiling, and in vivo proof-of-concept efficacy in acute pancreatitis. *J. Med. Chem.* **2018**, *61*, 9756–9783. (b) Pirali, T.; Riva, B.; Genazzani, A. A. Modulators of SOCE, Compositions and use thereof. WO 2017212414 A1, Dec 14, 2017.

(17) (a) Schleifer, H.; Doleschal, B.; Lichtenegger, M.; Oppenrieder, R.; Derler, I.; Frischauf, I.; Glasnov, T.; Kappe, C.; Romanin, C.; Groschner, K. Novel pyrazole compounds for pharmacological discrimination between receptor-operated and store-operated Ca²⁺ entry pathways. *Br. J. Pharmacol.* **2012**, *167*, 1712–1722. (b) Kiyonaka, S.; Kato, K.; Nishida, M.; Mio, K.; Numaga, T.; Sawaguchi, Y.; Yoshida, T.; Wakamori, M.; Mori, E.; Numata, T.; Ishii, M.; Takemoto, H.; Ojida, A.; Watanabe, K.; Uemura, A.; Kurose, H.; Morii, T.; Kobayashi, T.; Sato, Y.; Sato, C.; Hamachi, I.; Mori, Y. Selective and direct inhibition of TRPC3 channels underlies biological activities of a pyrazole compound. *Proc. Natl. Acad. Sci. U.S.A.* **2009**, *106*, 5400–5405.

(18) (a) Ng, S. W.; di Capite, J.; Singaravelu, K.; Parekh, A. B. Sustained activation of the tyrosine kinase Syk by antigen in mast cells requires local Ca²⁺ influx through Ca²⁺ release-activated Ca²⁺ channels. *J. Biol. Chem.* **2008**, *283*, 31348–31355. (b) Di Sabatino, A.; Rovedatti, L.; Kaur, R.; Spencer, J. P.; Brown, J. T.; Morrisset, V. D.; Biancheri, P.; Leakey, N. A. B.; Wilde, J. I.; Scott, L.; Corazza, G. R.; Lee, K.; Sengupta, N.; Knowles, C. H.; Gunthorpe, M. J.; McLean, P. G.; MacDonald, T. T.; Kruidenier, L. Targeting gut T cell Ca²⁺ release activated Ca²⁺ channels inhibits T cell cytokine production and T-Box transcription factor T-Bet in inflammatory bowel disease. *J. Immunol.* **2009**, *183*, 3454–3462. (c) Xie, Y.; Holmqvist, M.; Mahiou, J.; Ono, M.; Sun, L.; Chen, S.; Zhang, S.; Jiang, J.; Chimmanamada, D.; Fleig, A.; Yu, C.-Y. Method for Modulating Calcium Ion-Release-Activated Calcium Ion Channels. CN 1826121 A, Feb 03, 2005; (d) Xie, Y.; Holmqvist, M.; Mahiou, J.; Ono, M.; Sun, L.; Chen, S.; Zhang, S.; Jiang, J.; Chimmanamada, D.; Yu, C.-Y. Compounds for Inflammation and Immune-Related Uses. U.S. Patent 8,314,134 B2, Feb 3, 2005.

(19) Li, J.; McKeown, L.; Ojelabi, O.; Stacey, M.; Foster, R.; O'Regan, D.; Porter, K. E.; Beech, D. J. Nanomolar potency and selectivity of a Ca²⁺ release-activated Ca²⁺ channel inhibitor against store-operated Ca²⁺ entry and migration of vascular smooth muscle cells. *Br. J. Pharmacol.* **2011**, *164*, 382–393.

(20) (a) Bonandi, E.; Christodoulou, M. S.; Fumagalli, G.; Perdicchia, D.; Rastelli, G.; Passarella, D. The 1,2,3-triazole ring as a bioisostere in medicinal chemistry. *Drug Discovery Today* **2017**, *22*, 1572–1581. (b) Kumari, S.; Carmona, A. V.; Tiwari, A. K.; Trippier, P. C. Amide Bond Bioisosteres: Strategies, Synthesis, and Successes. *J. Med. Chem.* **2020**, *63*, 12290–12358.

(21) (a) Tron, G. C.; Pirali, T.; Billington, R. A.; Canonico, P. L.; Sorba, G.; Genazzani, A. A. Click chemistry reactions in medicinal chemistry: applications of the 1,3-dipolar cycloaddition between azides and alkynes. *Med. Res. Rev.* **2008**, *28*, 278–308. (b) Jiang, X.; Hao, X.; Jing, L.; Wu, G.; Kang, D.; Liu, X.; Zhan, P. Recent applications of click chemistry in drug discovery. *Expert Opin. Drug Discovery* **2019**, *14*, 779–789.

(22) Azimi, I.; Stevenson, R. J.; Zhang, X.; Meizoso-Huesca, A.; Xin, P.; Johnson, M.; Flanagan, J. U.; Chalmers, S. B.; Yoast, R. E.; Kapure, J. S.; Ross, B. P.; Vetter, I.; Ashton, M. R.; Launikonis, B. S.; Denny, W. A.; Trebak, M.; Monteith, G. R. A new selective pharmacological enhancer of the Orai1 Ca²⁺ channel reveals roles for Orai1 in smooth

and skeletal muscle functions. *ACS Pharmacol. Transl. Sci.* **2020**, *3*, 135–147.

(23) (a) Pagliai, F.; Pirali, T.; Del Grosso, E.; Di Brisco, R.; Tron, G. C.; Sorba, G.; Genazzani, A. A. Rapid synthesis of triazole-modified resveratrol analogues via click chemistry. *J. Med. Chem.* **2006**, *49*, 467–470. (b) Pirali, T.; Pagliai, F.; Mercurio, C.; Boggio, R.; Canonico, P. L.; Sorba, G.; Tron, G. C.; Genazzani, A. A. Triazole-modified histone deacetylase inhibitors as a rapid route to drug discovery. *J. Comb. Chem.* **2008**, *10*, 624–627.

(24) (a) Lolli, M. L.; Sainas, S.; Pippione, A. C.; Giorgis, M.; Boschi, D.; Dosio, F. Use of human dihydroorotate dehydrogenase (hDHODH) inhibitors in autoimmune diseases and new perspectives in cancer therapy. *Recent Pat. Anticancer Drug Discov.* **2018**, *13*, 86–105. (b) Leban, J.; Saeb, W.; Garcia, G.; Baumgartner, R.; Kramer, B. Discovery of a novel series of DHODH inhibitors by a docking procedure and QSAR refinement. *Bioorg. Med. Chem. Lett.* **2004**, *14*, 55–58. (c) Munier-Lehmann, H.; Vidalain, P.-O.; Tangy, F.; Janin, Y. L. On dihydroorotate dehydrogenases and their inhibitors and uses. *J. Med. Chem.* **2013**, *56*, 3148–3167.

(25) (a) Davis, J. P.; Cain, G. A.; Pitts, W. J.; Magolda, R. L.; Copeland, R. A. The immunosuppressive metabolite of leflunomide is a potent inhibitor of human dihydroorotate dehydrogenase. *Biochemistry* **1996**, *35*, 1270–1273. (b) Palmer, A. M. Teriflunomide, an inhibitor of dihydroorotate dehydrogenase for the potential oral treatment of multiple sclerosis. *Curr. Opin. Invest. Drugs* **2010**, *11*, 1313–1323.

(26) Rahman, S.; Rahman, R. Unveiling some FDA-approved drugs as inhibitors of the store-operated Ca²⁺ entry pathway. *Sci. Rep.* **2017**, *7*, 12881–12893.

(27) Peters, G. J.; Sharma, S. L.; Laurensse, E.; Pinedo, H. M. Inhibition of pyrimidine de novo synthesis by DUP-785 (NSC368390). *Invest. New Drugs* **1987**, *5*, 235–244.

(28) Sainas, S.; Pippione, A. C.; Lupino, E.; Giorgis, M.; Circosta, P.; Gaidano, V.; Goyal, P.; Bonanni, D.; Rolando, B.; Cignetti, A.; Ducime, A.; Andersson, M.; Järvä, M.; Friemann, R.; Piccinini, M.; Ramondetti, C.; Buccinnà, B.; Al-Karadaghi, S.; Boschi, D.; Saglio, G.; Lolli, M. L. Targeting Myeloid Differentiation Using Potent 2-Hydroxypyrazolo[1,5-a]pyridine Scaffold-Based Human Dihydroorotate Dehydrogenase Inhibitors. *J. Med. Chem.* **2018**, *61*, 6034–6055.

(29) Paterniti, I.; Mazzon, E.; Riccardi, L.; Galuppo, M.; Impellizzeri, D.; Esposito, E.; Bramanti, P.; Cappellani, A.; Cuzzocrea, S. Peroxisome proliferator-activated receptor β/δ agonist GW0742 ameliorates cerulein- and taurocholate-induced acute pancreatitis in mice. *Surgery* **2012**, *152*, 90–106.